

# Nanoscale

rsc.li/nanoscale



ISSN 2040-3372

## REVIEW

[View Article Online](#)  
[View Journal](#) | [View Issue](#)
Cite this: *Nanoscale*, 2024, **16**, 7264

# Printable and flexible integrated sensing systems for wireless healthcare

Kemeng Zhou,<sup>†</sup> Ruochen Ding,<sup>†</sup> Xiaohao Ma and Yuanjing Lin \*

The rapid development of wearable sensing devices and artificial intelligence has enabled portable and wireless tracking of human health, fulfilling the promise of digitalized healthcare applications. To achieve versatile design and integration of multi-functional modules including sensors and data transmission units onto various flexible platforms, printable technologies emerged as some of the most promising strategies. This review first introduces the commonly utilized printing technologies, followed by discussion of the printable ink formulations and flexible substrates to ensure reliable device fabrication and system integration. The advances of printable sensors for body status monitoring are then discussed. Moreover, the integration of wireless data transmission *via* printable approaches is also presented. Finally, the challenges in achieving printable sensing devices and wireless integrated systems with competitive performances are considered, so as to realize their practical applications for personalized healthcare.

Received 30th November 2023,  
Accepted 16th February 2024

DOI: 10.1039/d3nr06099c

[rsc.li/nanoscale](https://rsc.li/nanoscale)

## 1. Introduction

Sensors play a crucial role in converting targeted analytes into measurable electric signals, making them a vital tool in medical care and health monitoring.<sup>1–8</sup> The rapid development of a large library of functionalized sensors has enabled

the widespread utilization of wearable sensors over the past few decades.<sup>9–13</sup> In addition, wireless transmission technologies have evolved to achieve high-speed data transfer. The most widely used wireless technologies for wearable sensors are Radio Frequency Identification (RFID),<sup>14–16</sup> Near Field Communication (NFC),<sup>14,17,18</sup> and Bluetooth.<sup>19,20</sup> The combination of wearable sensors and wireless communication modules enables pervasive sensing and interconnection of physical objects *via* the wearable Internet of Things (IoT).<sup>21–23</sup> Integrated wireless sensor systems are qualified to collect data from subjects and the local environment and transmit them to remote devices for further data analytics and visualization.<sup>24,25</sup> These systems have a range of applications in health monitoring, environmental detection and artificial intelligence, bringing great convenience to human life.

Printing technologies, including screen printing, roll-to-roll (R2R) printing, inkjet printing and three dimensional (3D) printing, have been widely adopted to realize wearable sensing devices and antenna systems.<sup>26–34</sup> These printable fabrication procedures provide the advantages of relatively low cost, high throughput, and desirable compatibility with various functional materials and platforms. For instance, the antenna for near field communication (RFID) wireless data transmission can be prepared on textiles, plastics, and other substrates with versatile designs on antenna patterns in a straightforward manner using printing technologies. This approach enables the integration of wireless communication modules into wearable devices, providing new opportunities for real-time monitoring and data transmission.

School of Microelectronics, Southern University of Science and Technology, Shenzhen 518055, China. E-mail: [linyj2020@sustech.edu.cn](mailto:linyj2020@sustech.edu.cn)

<sup>†</sup>These authors contributed equally to this work.



Yuanjing Lin

*Yuanjing Lin received her Ph.D degree in Electronics and Computer Science from the Hong Kong University of Science and Technology in 2018. From 2019 to 2020, she was a Postdoctoral Fellow in Electrical Engineering and Computer Sciences at the University of California, Berkeley. She is currently an Assistant Professor at the Southern University of Science and Technology. Her research interests focus on nanomaterial*

*innovation for wearable and printable electronics, micro/nano-structured sensors, flexible energy storage devices and their applications in smart systems.*





**Fig. 1** The most commonly adopted technologies and electronic configurations for printable sensing systems with wireless data transmission. Screen printing. Reproduced from ref. 35 with permission from [Springer Nature], copyright [2020]. Roll-to-roll printing. Reproduced from ref. 36 with permission from [American Chemical Society], copyright [2018]. Inkjet printing. Reproduced from ref. 37 with permission from [John Wiley and Sons], copyright [2019]. 3D printing. Reproduced from ref. 38 with permission from [Elsevier], copyright [2022]. Physical sensors. Reproduced from ref. 39 with permission from [American Chemical Society], copyright [2019]. Chemical sensors. Reproduced from ref. 40 with permission from [Elsevier], copyright [2020]. An RFID tag. Reproduced from ref. 41 with permission from [Springer Nature], copyright [2022]. An NFC label. Reproduced from ref. 42 with permission from [John Wiley and Sons], copyright [2021].

This review focuses on recent research progress in printable sensing systems with wireless data transmission (Fig. 1). Section 2 provides an overview of printing technologies for wearable electronics. Section 3 discusses the commonly utilized printable materials and their unique properties, while section 4 provides a summary of printable substrates as wearable platforms. Afterwards, section 5 presents the recent advances in printable physical and chemical sensors and their applications for smart sensing. In section 6, the design and printable fabrication of antennas for wireless data transmission are discussed, followed by the advances of integrated wireless sensing systems for real-time and remote monitoring presented in section 7. Finally, section 8 discusses challenges and research prospects for printable sensing devices with wireless data transmission. The advances in printing technologies provide a cost-effective and versatile approach for the fabrication and integration of sensors and multifunctional modules for a wide range of applications, including healthcare, environmental monitoring, and smart cities.

## 2. Printable technologies for integrated sensing systems

Printing techniques have been widely employed in device fabrication and integrated systems for sensing applications. Printable sensing systems can be designed for various platforms with the attractive factors of versatile configuration, compatibility of different substrates and facile integration. This section provides a summary of the major printing methods for sensor devices, including screen printing, inkjet printing, R2R printing, and 3D printing technologies. In general, each printing method has unique properties, including printing speed, resolution, ink viscosity, printed film thickness and substrate adaptability. The selection of the appropriate printing method depends on the specific requirements of device fabrication, including the type of sensor, the substrate materials, and the desired properties. Table 1 provides a summary and comparison of the key factors for different printing technologies.<sup>43</sup>

**Table 1** Summary of the key factors for different printing techniques<sup>44–50</sup>

	Screen printing	R2R printing	Inkjet printing	3D printing
Resolution ( $\mu\text{m}$ )	>50	>0.05	>0.5	>30
Printing speed ( $\text{m min}^{-1}$ )	~70	~1000	~1	~4
Mask	Yes	Yes	No	No
Substrate geometry	Flat	Flat	Irregular	Irregular
Ink properties	High viscosity and shear thinning	Low viscosity	Low viscosity, long-term stability, and small particle size	Shear thinning, and low solvent content
Advantages	Fast fabrication, low-cost, and high-throughput	High printing speeds and high throughput	Precise control, low materials waste, and low-cost	High aspect ratios and printed layer thicknesses; 3D geometries
Disadvantages	Low-resolution	High cost and space requirement	Nozzle clogging and limited types of inks	Relatively low resolution

## 2.1. Screen printing

Screen printing is a popular printing process that uses porous stencils to transfer ink onto a substrate. The screen, squeegee, and substrate play key roles in the printing process. The printable area of the screen, usually made of porous mesh fabric and nylon, is always open, allowing ink to pass through, while the non-printable area is blocked off by a hardened photosensitive material.<sup>26,51,52</sup> The masks act as image carriers and ink metering systems throughout the printing process, setting

minimum feature sizes and deposition thicknesses. As shown in Fig. 2a, the printing inks are pressed down onto the substrates through the masks under squeegee pressure.<sup>53</sup>

Without strict requirements on the physical and chemical properties of the printing materials, screen printing provides superior compatibility for device fabrication on different flexible platforms. It is a versatile technology that can be used for large-scale production on different substrates, including fabrics and polymers. It is suitable for printing materials with high concentrations or large particle sizes. It serves as one of

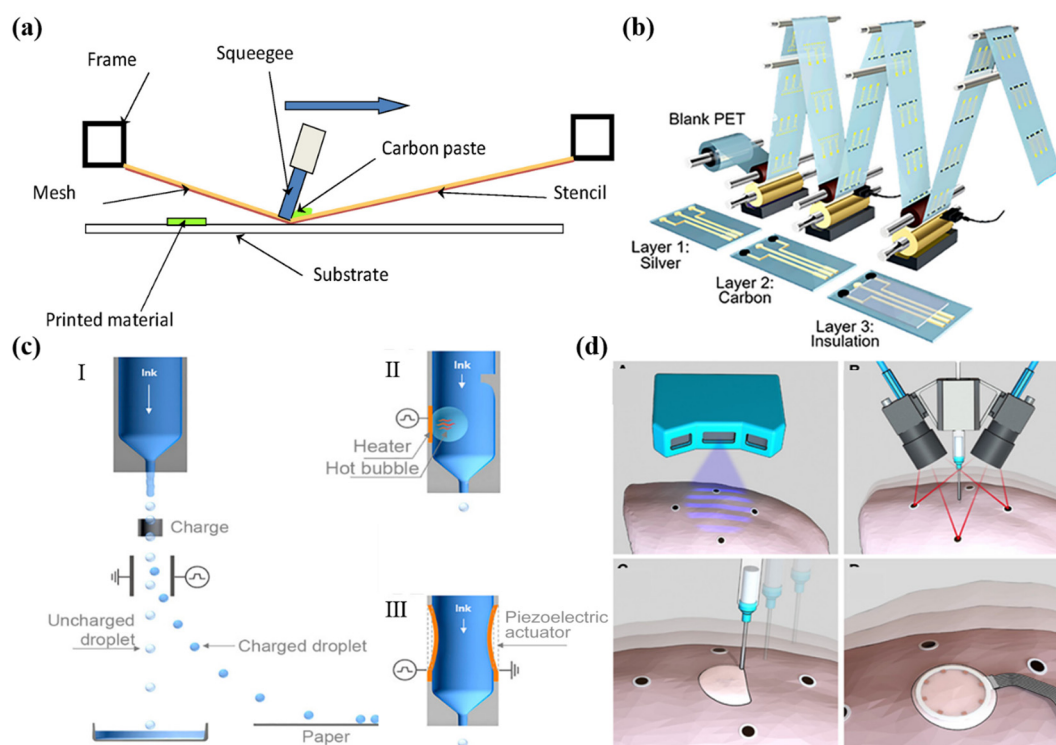


**Fig. 2** Printing technology of sensors. (a) Schematic demonstration of screen printing. Reproduced from ref. 53 with permission from [Elsevier], copyright [2016]. (b) R2R gravure printed electrochemical sensors. Reproduced from ref. 36 with permission from [American Chemical Society], copyright [2018]. (c) Continuous inkjet printing (I) and drop-on-demand inkjet printing (thermal inkjet (II) and piezoelectric inkjet (III)). Reproduced from ref. 66 with permission from [American Chemical Society], copyright [2020]. (d) Direct 3D printing of sensors on pig lungs. Reproduced from ref. 81 with permission from [American Association for the Advancement of Science], copyright [2020].

the most affordable and facile methods for preparing conductive electrode patterns and functional layers. Thus, it has been widely adopted for fabricating devices based on layer-by-layer thin-film architectures, such as sensors, batteries and optoelectronics. However, the disadvantages lie in the relatively high material waste and low patterning resolution, which limit the device performance enhancements, especially for those that require minimized patterning line width/interspacing and highly precise control of the film thickness. Besides, since it requires masks for patterning, and direct contact between the applied masks and printed layers is unavoidable, the construction of high performance sensing devices with strict requirements on the printed film quality and functional layer interfaces can be limited.

## 2.2. R2R printing

R2R printing is a typical solution-based process applied to large-scale and mass manufacturing of devices. It employs additive and subtractive processes to fabricate structures with high throughput and low cost.<sup>51,54,55</sup> Among different types of R2R printing processes, gravure and flexographic printing are two of the representative technologies to achieve high-throughput patterning.

In gravure printing, printed patterns are firstly constructed on the surface of the gravure cylinder in the form of an engraved intaglio grid, which is then directly transferred to substrates by physical contact ink deposition.<sup>56,57</sup> It allows pattern reproduction with variable depth and size, providing compatibility for a variety of substrates. In flexographic printing, functional inks are transferred to the anilox roller, followed by the removal of excess ink in the non-image area by blades. In this way, the pattern can then be completely transferred to the flexographic printing plate.<sup>57</sup> Compared to screen printing, R2R printing exhibits higher printing speeds, resolution, and fabrication reproducibility. Thus, it enables large scale and high-throughput patterns and device manufacture. For instance, Javey and Cho *et al.* demonstrated R2R gravure printing of electrodes on flexible substrates in a scale of up to 150 m. The as-printed electrodes showed remarkable consistency in conductivities, which can then be functionalized into sensors with reproducible performances for promising applications in health monitoring (Fig. 2b).<sup>36</sup> Lee *et al.* manufactured comb-structured acceleration sensors on PET in a scalable fashion by R2R gravure printing. The sensors are based on sandwich device architectures including the Ag bottom electrode, the barite barium sulfate (BaSO<sub>4</sub>) dielectric layer and the Ag top electrode. To avoid the stiction problem, the Ag top electrodes were printed on the water-soluble PVP sacrificial layer and then transferred on top of the dielectric layer.<sup>58</sup> Javey *et al.* achieved electrochemical sensors with remarkable performance reproducibility for wearable and medical devices *via* R2R printing.<sup>59</sup>

## 2.3. Inkjet printing

Inkjet printing is a non-contact printing technology that can be categorized into two main methods: continuous inkjet

printing (CIJ) and drop-on-demand (DOD) inkjet printing (Fig. 2c).<sup>60–66</sup> During CIJ printing, the nozzles continuously produce droplets, while in DOD inkjet printing, droplets are only ejected when the appropriate signal is received. DOD inkjet printing can generate pressure pulses that control the formation and ejection of inks.

To achieve the precise control of ink jetting during DOD, thermal and piezoelectric cartridges are commonly adopted. In thermal inkjet printing, the inks are heated by a heating element, which results in bubble formation followed by rapid expansion and collapse.<sup>67</sup> The bubble explosion creates the driving power that ejects the ink from the nozzle.<sup>64,65,68</sup> However, the high temperature process limits the choice of printing materials and substrates, and can also affect the printing stability and device performance. In contrast, piezoelectric inkjet printing applies voltage pulses to a piezoelectric actuator, which deforms the actuator and causes the nozzle to eject droplets.<sup>64,65,68–70</sup> By changing the pulse pressure, piezoelectric inkjet printers can realize the desirable precise control of the droplet speed. Normally the cartridges for inkjet printing allow droplets in the volumes of 1 pL to several tens of pL. Thus, piezoelectric inkjet printing exhibits desirable form factors of high patterning resolution, precise materials mass loading, enhanced ink stability and low pollution. Thus, it has been widely adopted for the fabrication of micro-sensors, in which high resolution electrodes and precise control of functional materials' mass loading play a critical role in ensuring high sensing performances. However, the printing speed can be relatively low compared to other methods, and thus might not be preferred for industrial level applications. Besides, to avoid nozzle clogging issues, it requires efforts on the synthesis of inks with rational optimized viscosity, high stability and uniform particle size. For instance, it normally requires low-viscosity inks with small particle sizes to ensure smooth printing, which to some extent limits the material's compatibility, such as nanowires and 2D materials.

## 2.4. 3D printing

3D printing is another type of drop-on-demand process in which materials are printed layer by layer in an additive manner based on digitally controlled material deposition. It has become increasingly popular for the fabrication of sensors attributed to its advantages of low material waste, mass fabrication, versatile customization, rapid prototyping, and facile procedures.<sup>71,72</sup> Among different types of 3D printing, direct ink writing (DIW), fused deposition modeling (FDM), selective laser sintering (SLS), stereolithography (SLA) are the most commonly adopted strategies.<sup>73–76</sup> Typically, DIW refers to the direct extrusion of a fluid material through a nozzle to form the desired shape, while FDM involves melting and extruding a thermoplastic filament through a nozzle to form the desired shape. Polymers and composite inks with high viscosities or that can be pre-synthesized into solid-state filaments are mainly utilized. To further broaden the material library for functional device construction and geometry resolution, laser-assisted 3D printing methods are introduced. SLS utilises

lasers to sinter powdered materials such as metals and polymers to form the desired shapes, while SLA realizes light sensitive materials that solidify a liquid layer by layer.

Attributed to the facile and versatile construction of irregular architectures, a variety of integrated sensing devices have been demonstrated.<sup>77–79</sup> For example, Kim and co-workers developed 3D-printed flexible sensors for ion sensing integrated into a flexible microfluidic patch for wearable sweat sensing.<sup>80</sup> Moreover, 3D printing allows direct device fabrication on non-planar substrates, such as biological surfaces. Recently, McAlpine *et al.* realized *in situ* 3D-printed sensors on porcine lungs for tissue surface deformation mapping based on electrical impedance tomography. Such an adaptive 3D printing approach provides an innovative strategy to construct implantable medical devices (Fig. 2d).<sup>81</sup>

### 3. Formulas of printable inks for sensing devices

The printable inks used for preparing sensors and integrated devices typically consist of solvents, functional micro/nano materials, conductive fillers, binders, and additives.<sup>60,82,83</sup> The solvents contribute to dissolving or dispersing active components and modifying the ink viscosity, while the binders minimize the intermolecular interaction between fillers, improving their stability and shelf life. Additives help prevent nanoparticle agglomeration, ensuring a smooth printing process. The functional conductive fillers largely affect the ink conductivity, which is one of the most critical factors for the performance enhancement of the printed devices. It is worth mentioning that the printable ink formula, especially the composition of functional materials and solvents, may differ widely depending on specific applications. For most printed sensors and integrated systems, decent conductivities of electrodes and interconnects are highly desirable to ensure electron transfer. Therefore, the most commonly used conductive fillers, including metal, carbon-based and conductive polymer materials, will be discussed in this section.

#### 3.1. Metallic inks

Metal inks are a popular choice for printed electrode contacts and interconnects due to their relatively higher electrical conductivity when compared to other types of inks.<sup>84</sup> There are various commercially available metallic-based inks based on silver (Ag), gold (Au), and copper (Cu), while the ink formulas can directly affect the electrical and mechanical properties of the printed sensor systems.

**Ag.** Ag-based inks are a popular choice for the conductive layer of sensors due to their excellent electrical conductivity and cost-effectiveness.<sup>85</sup> Silver nanoparticles (Ag NPs) and silver nanowires (Ag NWs) are the two typical materials used in silver-based inks.<sup>86–88</sup> Ag NP inks are one of the most commercially available printing materials mainly due to their ease of synthesis and can be formulated into a variety of rheological properties. It has been widely adopted for inkjet printing,

screen printing and R2R printing. The as-printed conductive electrodes might encounter decreased conductivity resulting from the loss of contact among the particles, especially under repeating bending. Thus, to realize highly conductive and flexible electrodes, Ag NWs are preferred. Xu *et al.* presented composite electrodes composed of inkjet-printed Ag NWs and PDMS. The optimized normalized resistance change of this stretchable electrode was as low as 4.67% in a 50% stretching test cycle.<sup>89</sup> One of the main challenges in the manufacturing process of silver inks lies in the aggregation of silver NPs and NWs into large particles. To prevent aggregation, stabilizers and binders are usually adopted in the optimized ink formulas. While for Ag NWs with high aspect ratios, it is more difficult to achieve uniform dispersion.<sup>86,90</sup> Another effective method can be ink sintering after printing to remove aggregated nanoparticles and nanowires so as to ensure continuous electron transfer and enhance the device performance.<sup>60,90–92</sup>

However, most of the flexible substrates cannot withstand high temperature processing. Research efforts have been devoted to investigating the potential methods to print Ag patterns with desirable conductivity without high temperature annealing.<sup>93</sup> Wu *et al.* developed Ag nanodendrites with a specific branching structure for printable inks (Fig. 3a).<sup>90</sup> The branching structure can form an interconnected network and allows sintering at a relatively low temperature of 80 °C to achieve high conductivity. This method would inspire the fabrication of printed sensors and integrated systems in a cost-effective and time-efficient manner, while minimizing the risk of flexible substrate damage.

**Au.** Despite being one of the most expensive conductive materials, Au exhibits excellent conductivity and chemical stability. In printable inks, Au conductive fillers can be engineered into typical morphologies such as nanoparticles, nanospheres, and nanowires.

The species and concentrations of reducing agents can affect the size, shape, and yield of gold nanoparticles.<sup>94,95</sup> It has been reported that starch molecules can be hydrolyzed to control further growth and produce gold nanoparticle solutions with controllable and stable sizes. The starch solution is heated and hydrolyzed in sodium hydroxide (NaOH) to activate its reducing end, which reduces the Au ions in the solution to Au<sup>0</sup>.<sup>95,96</sup> Based on this approach, Enriquez *et al.* realized stable and high yield synthesis of Au NPs by fine-tuning the size of starch granules, coupled with microwave-assisted synthesis (Fig. 3b).<sup>95</sup> Another classic approach to prepare Au fillers with controllable morphologies is the seed-mediated growth method, in which Au<sup>3+</sup> ions are normally reduced by sodium citrate.<sup>97</sup> Mazali *et al.* adopted the seed-mediated approach for preparing Au nanosphere colloids with high uniformity.

To reduce the cost, Au-based composite inks provide alternative choices. He *et al.* recently developed a convenient method for growing highly conductive gold nanowires on carbon nanofibers (CNFs).<sup>98</sup> By regulating the reduction kinetics of Au(III) precursors and preventing nanoparticle fusion, Au nanocrystals undergo monomer-by-monomer attachment of Au (0) monomers onto the facets of Au crystals, resulting in





**Fig. 3** Preparation strategies of conductive printable inks. (a) Silver-based ink (Ag ND) with a special branch structure. Reproduced from ref. 90 with permission from [the Royal Society of Chemistry], copyright [2019]. (b) Microwave heating was used for both the controlled starch hydrolysis and AuNP synthesis. Reproduced from ref. 95 with permission from [American Chemical Society], copyright [2018]. (c) The non-equilibrium plasma transforms the metal ink into a metal structure at low temperatures. Reproduced from ref. 37 with permission from [John Wiley and Sons], copyright [2019]. (d) A high-concentration conductive ink based on defect-free graphene through a scalable hydrodynamic process. Reproduced from ref. 115 with permission from [Springer Nature], copyright [2021]. (e) Stable and biocompatible CNT ink stabilized by sustainable silk sericin. Reproduced from ref. 117 with permission from [John Wiley and Sons], copyright [2020].

the formation of a single-crystalline structure on CNFs. The resulting Au NW/CNF inks also show remarkable conductivity and stability for printable device fabrication.

**Cu.** Due to the relatively lower cost, copper nanoparticles can serve as a substitute for silver and gold nanoparticles. However, environmental oxygen exposure during storage,

printing and sintering can cause rapid oxidation of copper nanoparticles, hindering their wide applications in printed materials.

To address this issue, the oxidation resistance of Cu NPs can be improved by isolating the copper core from oxidizing substances with an oxidation-proof shell.<sup>99–103</sup> Jeong *et al.*

enhanced the chemical resistance of Cu NP particle membrane-based electrodes by covering the surface of Cu NPs with a Ni protective shell.<sup>104</sup> The electrical conductivity and oxidation resistance of the Cu@Ni electrode were improved by varying the thickness of the Ni shell. In addition to the Cu–Ni core–shell structure, the Cu–Ag core–shell structure has also been synthesized to prevent the oxidation of Cu particles.<sup>105</sup>

In general, the metal nanoparticles have a high particle density and surface free energy, which can lead to ink agglomeration. Thus, it is a common practice to apply stabilizers to prepare homogeneous inks.<sup>37</sup> Alternatively, particle-free inks with better storage stability might need to reduce the precursors to metals by thermal annealing after the printing process. However, the annealing could potentially deform the substrate.<sup>86,106</sup> To tackle this challenge, Zorman *et al.* have developed an inkjet printing technique that uses particle-free inks made from inorganic metal salts. These inks are transformed into metallic structures by nonequilibrium plasma at low temperatures (138 °C), as depicted in Fig. 3c.<sup>37</sup> Electrons from the plasma or secondary electrons released from the thin film reduce the metal cations to crystallize the metal. When metal salts are dissociated in the presence of ions, metal cations become available.

### 3.2. Carbon-based materials

Carbon-based materials, particularly graphite, graphene, and carbon nanotubes (CNTs), provide considerate and tunable conductivity, as well as superior chemical stability. Thus, tremendous research efforts have been devoted to the development of carbon-based ink formulas for multi-functional printable electronics.

**Graphene.** Graphene as a two-dimensional carbon material serves as a widely utilized ink substance for developing printed electronics due to its high electrical conductivity, chemical and thermal stability, and mechanical robustness.<sup>107–109</sup> The most commonly used methods to prepare printable graphene inks are liquid phase exfoliation (LPE) and electrochemical exfoliation.<sup>110,111</sup> However, these methods have limitations, such as low productivity, long fabrication time, and low graphene concentration.<sup>112,113</sup>

To address these issues, hydrokinetic-based graphite exfoliation methods were applied to directly exfoliate graphite using suitable solvents and water to produce defect-free graphene sheets with large lateral dimensions.<sup>112,114</sup> Based on such scalable hydrodynamic strategies, Choi *et al.* developed a conductive ink based on defect-free graphene with a high-concentration of 47.5 mg mL<sup>−1</sup> (Fig. 3d).<sup>115</sup> Besides, electrochemical exfoliation is also a commonly adopted method for preparing graphene. Parvez *et al.* recently demonstrated a water-based inkjet printable ink made from electrochemically exfoliated graphene (ECG) in a time-efficient manner.<sup>116</sup> The inkjet printable inks containing more than 75% monolayer and multilayer graphene flakes were achieved using a core electrochemical stripping method. Two graphite foils as the anode and cathode were biased at a direct current (DC) voltage of 10 V for stripping in a 0.5 M (NH<sub>4</sub>)<sub>2</sub>SO<sub>4</sub> electrolyte. These

methods contribute to the synthesis of high-quality graphene inks for printed electronics.

**CNTs.** CNTs are one-dimensional materials in the specific structure of concentric circular tubes with several to tens of carbon atom layers. However, CNTs are difficult to disperse in the liquid phase due to solid  $\pi$ – $\pi$  interactions, leading to dense aggregation.

By introducing functional groups to the CNT surface or as reaction sites for subsequent modifications, CNTs can be dispersed in water and organic solvents with improved uniformity. Zhang *et al.* used silk sericin as a stabilizer to prepare stable and biocompatible CNT inks (Fig. 3e).<sup>117</sup> The formation of sericin–CNT hybrids with a core–sheath structure modifies the surface properties of CNTs and stabilizes their homogeneous dispersion. The prepared inks deliver decent compatibility to various printing methods and substrates. Mariatti *et al.* prepared stable and environmentally friendly water-based inks by dispersing multi-walled carbon nanotubes (MWCNTs) in an aqueous solution with the help of biopolymer surfactants Gum Arabic (GA).<sup>118</sup> The hydrophobic tail of GA adsorbs on the surface of MWCNTs, and the hydrophilic end extends into the water. Thus, the barrier between nanotubes can be formed to reduce aggregation.

In summary, carbon-based materials offer desired electrical conductivity and chemical inertness, enabling wide applications in composite ink formulas to construct printed electrodes for a variety of sensors.

### 3.3. Conductive polymer materials

Conductive polymers are another commonly adopted material for sensor fabrication due to their feasibility for preparing various printable formulations and functionalization *via* doping. Among various conductive polymers, poly(3,4-ethylenedioxythiophene):poly(styrene sulfonate) (PEDOT:PSS), and polyaniline (PANI) are two of the most commonly utilized materials in the construction and design of flexible and stretchable electrodes. Given their desirable biocompatibility, and electrical conductivity, together with reliable mechanical and electrochemical stability, a variety of printable inks for flexible sensing device and system fabrication have been reported.<sup>50,119–122</sup>

**PEDOT:PSS.** PEDOT:PSS consists of positively charged PEDOT coupled with the negatively charged insulator PSS polyelectrolyte. The PSS groups contribute to the increased charge carrier density of PEDOT, and the hydrophilicity of PSS stabilizes the dispersion of PEDOT chains in aqueous solutions.<sup>123</sup> Shapter *et al.* demonstrated an approach to achieve high-resolution and scalable printing of PEDOT:PSS *via* R2R printing.<sup>124</sup> The homogeneous PEDOT:PSS ink was prepared using a water/ethanol/solvent mixture to facilitate ink patterning and ensure high conductivity. Shao *et al.* employed screen printing to fabricate strain-humidity sensors with natural rubber latex (NRL) and PEDOT:PSS (30 wt%) composite inks.<sup>125</sup> The strain sensor demonstrated reliable performance under 10% strain for 500 cycles, making it applicable for monitoring various body movements. Simultaneously, the humidity sensor dis-



played a response time of 0.72 seconds and a detection range spanning from 6% to 83%, rendering it suitable for tracking human respiration and respiratory frequency. Du *et al.* also prepared a screen printing ink for strain sensor fabrication by incorporating 20 wt% PEDOT:PSS into PDMS.<sup>126</sup> The strain sensor for monitoring the movement of body joints can endure 10 000 cycles at 30% strain. Apart from these, PEDOT-based inks have been used for conductive interconnects for multi-functional device/chip integration.<sup>127–130</sup>

**PANI.** PANI provides the attractive properties of tunable electrical conductivity and multiple oxidation states, which make it popular especially for electrochemical device fabrication. PANI exhibits three structures based on different oxidation states, namely the leucoemeraldine base (LEB) form, emeraldine base (EB) form and pernigraniline base (PAB) form. The LEB represents the completely reduced state and appears white. The EB represents the semi-oxidized state and shows green. The PAB represents the fully oxidized state and turns darkish.<sup>131</sup> One of their most frequent applications is for pH sensing.<sup>132–135</sup> For instance, Monsalve *et al.* demonstrated a pH sensor based on screen printed carbon electrodes functionalized with inkjet printed PANI for sweat analysis. The sensor exhibited a sensitivity of 69.1 mV pH<sup>−1</sup> that fits with the Nernst equation.<sup>136</sup> Gabriel *et al.* proposed an ink formulation consisting of a PANI:PSS/(polypyrrole) PPy:PSS mixture and utilized inkjet printing to deposit the ink onto Au-phthalocyanine electrodes for pH sensors.<sup>137</sup> The interaction between PANI:PSS/PPy:PSS and Au-phthalocyanine resulted in the formation of delocalized  $\pi$  regions, enhancing the electron mobility and increasing the sensor performance. The pH sensor demonstrated a wide linear response range from pH 3 to 10, showcasing a remarkably high sensitivity of 81 mV pH<sup>−1</sup>.

## 4. Flexible substrates for printable electronics

One of the most attractive advantages of printable electronics lies in their capability to various flexible substrates. To realize high-performance electronics, it requires careful matching of printing techniques, printable inks and rationally modified surface properties of the flexible substrates. In this section, recent advances in preparing printable sensors on different flexible substrates and platforms will be discussed.

### 4.1. Polymer substrates

Flexible substrates based on polymers such as polyethylene terephthalate (PET), polyimide (PI) and stretchable elastomers are the most widely adopted platform for flexible and wearable electronics. This is mainly due to their relatively smooth surface morphologies and tunable properties for precise pattern printing, as well as excellent robustness and deformability.

Printable sensors for temperature, pressure, and electrochemical analyte monitoring have been well developed on PET substrates. For instance, Javey *et al.* realized high-throughput

fabrication of sensor electrodes, microchannel patterned spacers and packing layers based on PET substrates by combining R2R printing and laser cutting. By stacking the three layers vertically, sweat sensing patches can be prepared in a facile manner (Fig. 4a).<sup>59</sup> The prepared microfluidic sensor patch can be applied to real-time monitoring of the sweat rate and analytes such as sodium, potassium and glucose, which can provide critical information for personalized healthcare. While the fabrication strategies for printable sensors and systems on PET are quite mature, the flexible patches suffer from non-stretchable and less conformal contact with skin.

Stretchable elastic substrates provide enhanced mechanical stability to withstand deformation and improved skin contact comfort, which are particularly desired for E-skin sensing applications. Among various elastic substrates, polydimethylsiloxane (PDMS) with excellent flexibility, chemical resistance, and heat resistance emerges as one of the popular choices. It also shows good compatibility with different printing methods and inks, enabling versatile electrodes and sensing array fabrication. For instance, piezoresistive strain sensor arrays with high sensitivity can be prepared on an R2R patterned stretchable PDMS-Ag substrate with inkjet printed CNTs as sensing layers (Fig. 4b).<sup>138</sup> Wang *et al.* prepared PDMS-based sensors for wearable electrocardiography (ECG) and photoplethysmography (PPG) through inkjet printing, which can clearly detect the pulsating nature of blood in the tissue.<sup>127</sup>

Apart from these, other polymer-based substrates, including polyimide (PI), thermoplastic polyurethane (TPU),<sup>139</sup> and Kapton,<sup>140</sup> have also been utilized as flexible platforms for printable sensors. For instance, ultra-thin and adhesive commercial medical tapes can serve as skin-conformable substrates for sensor integration. These medical tapes are normally made of a thin polyurethane (PU) film coated with an acrylic adhesive and can be seamlessly applied on the human skin. By using aerosol jet printing to allow lower temperature sintering of the silver nanoparticle ink, Yeong *et al.* prepared a wearable strain sensor on such medical tapes to realize efficient capture of strain response signals from the body (Fig. 4c).<sup>141</sup> The printed sensors exhibit remarkable stability during repeated bending and stretching, which shows promising potential for remote clinical applications.

### 4.2. Textiles

Textiles are considered as one of the competitive candidates for skin-friendly sensing devices due to their flexibility and permeability with superior wearing comfort. Textiles are typically categorized into fibers, yarns, and fabrics. Fibers, with high length to diameter ratios, can be twisted to form threads or yarns.<sup>142</sup> Fabrics are defined as layered structures of fiber materials made from yarns, utilizing techniques such as weaving and knitting. Various conductive materials, including metals, conductive polymers, and carbon materials, have been employed to produce conductive fibers, which can then be further functionalized into sensing devices. To prepare textile-based sensors in a printable manner, screen printing is the commonly adopted approach. Mao *et al.* prepared e-textiles



**Fig. 4** The substrate of the print sensor. (a) The sweat sensor is fabricated on the PET substrate by R2R printing. Reproduced from ref. 59 with permission from [American Association for the Advancement of Science], copyright [2019]. (b) R2R printing technology prepares a highly sensitive piezoresistive strain sensor on a PDMS substrate. Reproduced from ref. 138 with permission from [American Chemical Society], copyright [2021]. (c) Wearable strain sensor on a medical bandage. Sensors based on medical bandages have good stability in 700 cycles of repeated bending and stretching. Reproduced from ref. 141 with permission from [American Chemical Society], copyright [2019]. (d) Screen-printed preparation of a multi-responsive fabric sensor with photochromic and thermochromic capabilities. Reproduced from ref. 35 with permission from [Springer Nature], copyright [2020]. (e) Screen-printed washable tribo-sensors on textiles for intelligent human-machine interactions. Reproduced from ref. 143 with permission from [American Chemical Society], copyright [2018]. (f) The high-sensitivity paper temperature sensor can be carried as a bar thermometer. The sensor is suitable for the human body's wearable health monitoring. Reproduced from ref. 144 with permission from [Elsevier], copyright [2020].

with photochromic, thermochromic, and ammonia sensing functionalities by screen-printing a viologen polymer made from cyclotriphosphazene onto cotton textiles (Fig. 4d).<sup>35</sup>

While screen printing provides a facile and scalable strategy to prepare sensors on textiles, it is found that the printed dense layers would sacrifice the air and moisture permeability of the textiles. Moreover, the relatively high viscosity of screen printing inks could bind the fibers into bundles and lead to cracks or materials delamination with mechanical interfer-

ences. Utilizing active materials to form interaction with the fibers can be a promising approach to realize e-textiles with mechanical stability under harsh deformation or even the washing process. Wang *et al.* demonstrated screen printed triboelectric touch/gesture sensing textile based CNTs (Fig. 4e).<sup>143</sup> Due to the interaction between CNTs and fiber networks, the e-textiles display desirable sensitivity for intelligent human-machine interfacing application, while maintaining permeability and washability.

Another concern for printable sensor fabrication on textiles lies in the limited patterning resolution mainly due to the capillary effects along the rough fiber surfaces and networks, which hinder device miniaturization and integration with microelectronic modules. It remains a challenge to achieve high-resolution and versatile patterning on textiles while maintaining their permeability and flexibility. Recently, Ma and co-workers reported a monolithically integrated in-textile sensing wristband by combining polymer-assisted metal deposition and the optimized lithography method with printed masks.<sup>12</sup> The developed integrated system in a single piece of textile consists of multifunctional modules, including the ion-selective sensor, signal processing circuit and Bluetooth wireless transmission, so as to realize epidermal sweat biosensing. The proposed strategy would provide a new perspective for textile sensing bioelectronics.

Overall, textiles offer a skin-friendly flexible platform for sensing devices with their original porous structure, permeability, and wearing comfort. To realize practical applications in wearable fitness monitoring and point-of-care healthcare, research efforts are expected to further enhance the patterning resolution and reliable encapsulation. Thus, e-textiles could exhibit competitive electrical conductivity, mechanical robustness and waterproofness compared to other flexible devices.

#### 4.3. Paper-based substrates

Paper has the advantages of low price, light weight, biodegradability, and recyclability. Most importantly, its surface roughness lies between polymers and textiles which makes it the most widely used platform for printing with a long history.<sup>144,145</sup> Lee *et al.* prepared sensors on paper that can simultaneously measure relative humidity, temperature, and compression bending through inkjet printing.<sup>144</sup> This high-sensitivity temperature sensor is suitable for use in smart packaging labels and disposable biosensors, and can also be carried around as a band thermometer (Fig. 4f). Impressively, the paper-based sensor shows a temperature sensing sensitivity of up to  $658.5 \Omega \text{ } ^\circ\text{C}^{-1}$ . The research advances in paper-based printable electronics will no doubt contribute to the wide applications of cost-effective and disposable sensors, especially for clinical quick tests.

However, papers normally cannot withstand stretching/twisting, and could have severe deformation with moisture/liquid. Therefore, rational packing designs are necessary for practical uses.

## 5. Printable sensors for bio-signal acquisition

With proper matching of printing methods, functional inks and flexible substrates, multifunctional sensors for bio-signal acquisition can be constructed in versatile designs. Similar to sensors prepared in conventional methods, printable sensors can also be categorized into physical and chemical sensors.

### 5.1. Physical sensors

Physical sensors are devices that utilize specific physical phenomena to convert the physical quantities being measured into electrical signals. The linear correlation between the input and output signals can be used for signal decoding. In this section, we will mainly discuss pressure, strain and temperature sensors, which are the most widely frequently reported printable sensors.

Pressure sensors can be applied for human activity tracking which can be estimated with the regional pressure and strain variations. 3D-printed hydrogel pressure sensors have been extensively researched due to their ease of preparation, excellent sensitivity, and mechanical strength. Guo *et al.* utilized a hydrogel with a self-healing function to create a 3D-printed sensor capable of monitoring human movement (Fig. 5a).<sup>146</sup> The hydrogel exhibited excellent self-healing function, remarkable stretchability, and stable recovery characteristics. Apart from the unique self-healing properties, other attractive factors of hydrogel sensors include biocompatibility, while the water loss could affect the sensor stability. Thus, skin-friendly and moisture-absorbing 3D-printed hydrogel pressure sensors that prevent water loss and preserve its performance are highly desirable. Yin *et al.* designed an ionic conductor through 3D printing (Fig. 5b).<sup>147</sup> The highly transparent, stretchable, and elastic hydrogel was then transformed into a capacitive sensor capable of detecting pressure and strain.

Another practical application of flexible pressure sensors is for health monitoring such as pulse sensing. The pulse waveform includes shock waves (P waves), tidal waves (T waves), and diastolic waves (D waves). Flexible pressure sensors applied onto human skin can extract the output variation under different pulse waves from deep tissues and distant sites, such as the digital artery and dorsalis pedis artery.<sup>148,149</sup> Due to the relatively small pressure signals generated by pulses, highly sensitive pressure sensors are required. Cheng *et al.* developed a pressure sensor with a fast response time and high sensitivity by combining inkjet printed Ag NP electrodes and conductors using a special pyramidal microarray structure (Fig. 5c).<sup>39</sup> The pressure sensor can detect arterial pulses and is suitable for wearable bio-diagnostics and therapy. Changes in deformation and pressure alter the contact area between the conductor and the printed electrodes of the pyramidal structure, resulting in a distinct signal response.

Apart from pulse sensing, motion tracking is another key application for flexible and printable sensors. Strain sensors can monitor the structural strain changes during human activities. For example, Tokito *et al.* fabricated a fully printed flexible strain sensor based on ferroelectric polymers. The sensor was utilized for wearable bending sensing on human fingers.<sup>150</sup> Zhang *et al.* patterned flexible strain sensors using MWCNTs/PDMS composite ink through screen printing. The printed sensors exhibited a high gauge factor of 1.55, demonstrating excellent linearity of up to 100% deformation. The sensors showcased robust sensing stability, and rapid dynamic



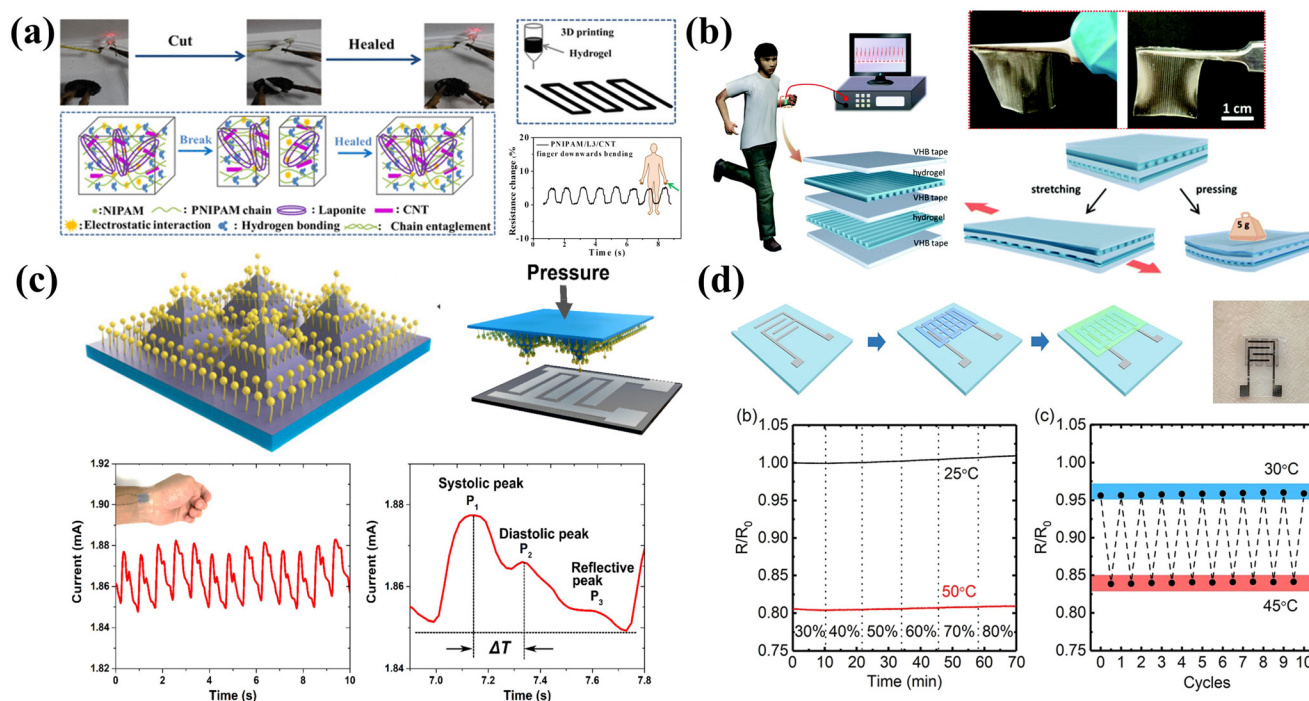


**Fig. 5** Printable physical sensors for human activity and health monitoring. (a) The self-healing hydrogel is used to prepare a pressure sensor that can monitor human movement through 3D printing. Reproduced from ref. 146 with permission from [American Chemical Society], copyright [2019]. (b) A high-sensitivity ion skin sensor was designed by 3D printing. Reproduced from ref. 147 with permission from [Royal Society of Chemistry], copyright [2019]. (c) Pressure sensor based on inkjet printed Ag NP electrodes and a special pyramid microstructure. Reproduced from ref. 39 with permission from [American Chemical Society], copyright [2019]. (d) Fully printed temperature sensor with a wide sensing range. Reproduced from ref. 153 with permission from [Springer Nature], copyright [2020].

response, enduring over 4000 strain cycles without degradation. These strain sensors are employed in wearable electronic devices for applications such as motion detection, exercise and rehabilitation training, as well as structural health monitoring.<sup>151</sup>

Temperature sensors fabricated *via* printing methods have also gained widespread attention due to the soaring demand, especially during the pandemic. Huang *et al.* proposed a strategy for the direct synthesis of molybdenum disulfide (MoS<sub>2</sub>) patterns on a polymer substrate using inkjet printing. The patterned MoS<sub>2</sub> serves as a temperature sensor for accurate epidermal temperature tracking.<sup>152</sup> Wang *et al.* developed a fully printed temperature sensor with a detection range of 25 °C to 50 °C and remarkable humidity stability (Fig. 5d).<sup>153</sup> The addition of a (3-glyceroyloxypropyl) trimethoxysilane (GOPS) crosslinker and fluorinated polymer passivator (CYTOP) significantly improved the humidity stability and temperature sensitivity of the PEDOT:PSS base membrane. By integrating printed sensors into the printed flexible hybrid circuit, real-time body temperature monitoring was achieved in a stable and reliable manner.

## 5.2. Chemical sensors

Chemical sensors are typically used for gas detection and biomarker analysis and convert analyte concentrations into quantified current or voltage signals.<sup>154</sup> Chemical sensors have

been widely applied in clinical medicine, environmental monitoring, biotechnology, the food industry and agriculture.<sup>5,155</sup>

Printable fabrication of chemical sensors can provide the desirable scalability, reproducibility and cost-effectiveness, especially for disposable rapid biosensing strips. One of the most widely adopted printed platforms for chemical detection in liquid samples is the screen printed three-electrode PET patch. It normally consists of two carbon-based patterns as working and counter electrodes, and one Ag pattern serves as the reference. One of the carbon-based electrodes can be functionalized with bio-receptors and other active materials so as to achieve selective and sensitive analyte detection.

A variety of printable chemical sensors for on-site rapid drug sensing, such as fentanyl, have also been reported on screen printed platforms, which can be prepared in a scalable manner (Fig. 6a).<sup>156</sup> In another work, Wang *et al.* presented a wearable electrochemical sensor device for rapid on-site saliva testing (Fig. 6b).<sup>40</sup> The device included shared counter and reference electrodes, and two printed selective sensing electrodes for dual analyte detection. Both THC and alcohol can be detected in saliva samples within three minutes with the printable sensing patch, demonstrating their potential applications in roadside driver screening.

Nevertheless, printable sensors normally exhibit non-competitive sensitivity and stability. One of the main reasons is limited surface areas with printed layers in the thin film mor-

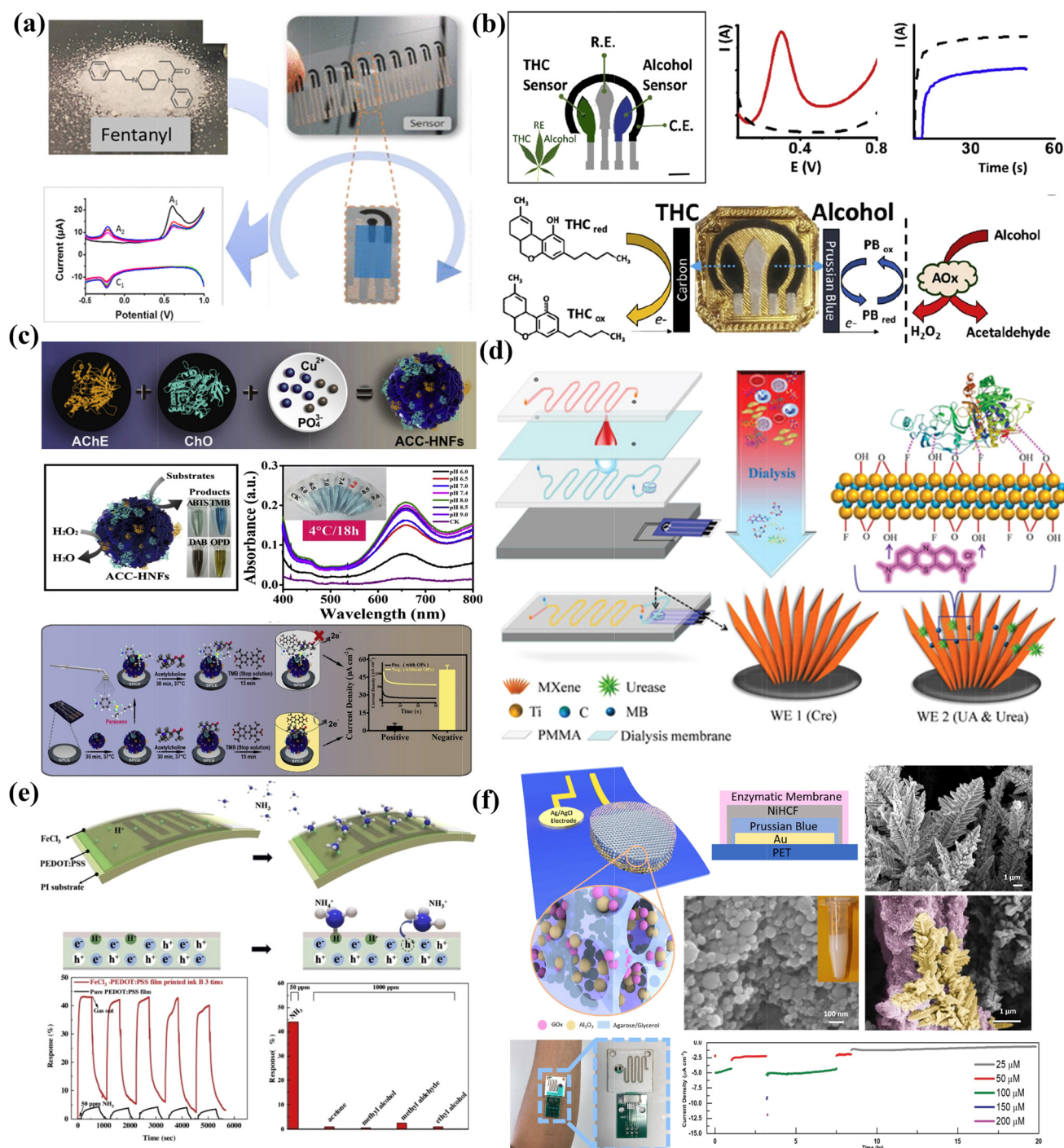


**Fig. 6** Printable chemical sensors for analytes' rapid/on-site testing and their performance enhancements with nanomaterials. (a) Scalable fabrication of on-site illegal drug fentanyl sensors. Reproduced from ref. 156 with permission from [American Chemical Society], copyright [2019]. (b) Saliva sensing patch for on-site THC and alcohol dual analyte detection. Reproduced from ref. 40 with permission from [Elsevier], copyright [2020]. (c) Paper-based organophosphorus pesticide sensor with ultrasensitivity based on enzyme-inorganic hybrid nanoflowers and can generate electrochemical/colorimetric signals simultaneously. Reproduced from ref. 157 with permission from [Elsevier], copyright [2019]. (d) MXene-based screen-printed electrodes with a dialysis microfluidic chip for blood analytes monitoring without extra pretreatment. Reproduced from ref. 158 with permission from [John Wiley and Sons], copyright [2018]. (e) Inkjet printing of a PEDOT:PSS thin film with FeCl<sub>3</sub> additives for high performance ammonia gas sensing. Reproduced from ref. 159 with permission from [Elsevier], copyright [2019]. (f) Nanostructured glucose sensor with reliable long-term stability prepared on printed sweat sensing platforms. Reproduced from ref. 154 with permission from [John Wiley and Sons], copyright [2019].

phology. It fails to facilitate interaction between analytes and sensitive materials, and the rapid charge accumulation at the interfaces would also lead to signal drifting. The other possible reason is that printed dense films can be easily delaminated especially in liquid sample analysis, which leads to device failures. Thus, it requires efforts to develop printable sensors with high sensitivity and stability for reliable and continuous sensing, such as portable contamination detection and wearable healthcare.

Researchers have proposed innovative printable strategies to combine with nanomaterials as to construct sensing devices for real-time and continuous biomarker monitoring with high accuracy and reliability. For example, Lu *et al.* successfully designed all-in-one enzyme-inorganic hybrid nanoflowers and immobilized on paper-based printed electrodes for on-site organophosphorus pesticide analysis. The sensor is capable of dual signal readings, including the electrochemical current output and colorimetric response, and delivers ultrahigh sensitivity (Fig. 6c).<sup>157</sup> Zhang *et al.* combined MXene-Ti<sub>3</sub>C<sub>2</sub>Tx-based screen-printed electrodes with a dialysis microfluidic chip to continuously monitor uric acid, urea, and creatine in human blood without extra pretreatment (Fig. 6d).<sup>158</sup> Attributed to the intriguing behavior of MXene nanosheets and the ratiometric sensing design to eliminate the signal drift caused by interferences, reliable and interference-free simultaneous quantification of the multiple biomarkers was validated to fulfill clinical and civil demands. In another work on gas sensing, Tan *et al.* developed a room-temperature ammonia gas sensor by inkjet printing (Fig. 6e).<sup>159</sup> By introducing FeCl<sub>3</sub> additives into the PEDOT:PSS thin film, the response signals increased by ten times with a corresponding 30-fold reduction in response time. To realize long-term continuous monitoring, Lin *et al.* combined printing and electrochemical fabrication strategies to develop nanotextured electrochemical enzymatic sensors for sweat glucose monitoring for up to 20 hours (Fig. 6f).<sup>154</sup> By taking advantage of the large surface areas that provide unique dendritic structures and conformal materials deposition, the sensitivities can be largely enhanced while the signal drift can be effectively suppressed compared with thin film sensors.

Overall, printable chemical sensors provide promising cost-effective approaches for on-site rapid testing of drugs, viruses/pathogens and other types of hazardous and toxic substances. By optimizing the printable ink formulas based on nanomaterials, and innovative combination of different nanoengineering strategies, it is expected that the sensing performance of printable sensors could be significantly enhanced. Thus, the requirements of various portable and wearable platforms for personalized healthcare and biomedical management can be fulfilled.

In summary, printable sensors that can be compatible and integrated into flexible platforms play a critical role in a wide range of applications, including medical diagnostics, health management, environment monitoring, the food industry, *etc.* The following table summarizes some of the representative works on printable sensors (Table 2).

## 6. Printable antennas for bio-signal transmission

Compared to conventional antennas on rigid platforms, the utilization of printable antennas in flexible devices for remote tracking enables miniaturization and reduces the weight of the wireless communication modules.<sup>170</sup> Some of the key factors for the design of antenna patterns mainly include the gain, operational frequency/bandwidth, and quality factor that indicate the energy loss rate (*Q*), impedance (*S*<sub>11</sub>), and weight. This section aims to elucidate the various types of commonly adopted antennas, including RFID, NFC, and specialized antennas. Moreover, a detailed examination of their distinctive properties and inherent advantages will be presented, thereby offering a comprehensive understanding of their role in wireless sensing technology.

### 6.1. RFID

In a typical RFID system, the digital information that is primarily storage in the RFID tag can be transmitted to readers by utilizing radio waves. It has been widely used in the IoT industry for convenient item tracking. To realize high performance printable antennas with lightweight and mechanical robust-

**Table 2** Printable sensors with their typical applications and performances

Printing method	Target analyte	Application	Sensitivity	Linear range	Detection limit	Ref.
Screen printing	Ammonia/formaldehyde	Gas monitoring	—	—	0.6 ppm/2.9 ppm	160
	Glucose	Blood glucose monitoring	143 $\mu\text{A mM}^{-1} \text{ cm}^{-2}$	1 $\mu\text{M}$ –11 mM	0.48 $\mu\text{M}$	161
	Hydroxylamine	Water monitoring	—	0.007–385.0 $\mu\text{M}$	2.0 nM	162
R2R	pH	Food packaging	55.5 mV pH <sup>-1</sup>	—	—	163
Inkjet printing	C-reactive protein	Immunoassay	2 $\mu\text{g mL}^{-1}$	—	—	164
	Lactate	Intensive care	8.86 nA mM <sup>-1</sup>	0.6–2.2 mM	—	165
	Pressure	Wearable electronic applications	0.48 kPa <sup>-1</sup>	—	—	166
3D printing	Methyl Viologen	Pesticide paraquat monitoring	—	3.0–100 $\mu\text{M}$	0.80 $\mu\text{M}$	167
	Temperature	High-temperature monitoring	28.3 pm K <sup>-1</sup>	—	—	168
	Pressure	Smart insole	1.19 MPa <sup>-1</sup>	0–872.4 kPa	—	169



ness for versatile integration with products, there is growing interest in leveraging two-dimensional (2D) materials such as graphene for antenna fabrication, owing to their exceptional electrical, mechanical, and thermal properties, as well as their high surface-to-volume ratio. Delipinar *et al.* demonstrated the development of textile-based RFID tags using spray, dispense, and contact printing processes of graphene.<sup>171</sup> These graphene textile RFID tags exhibited induced voltages that render them highly suitable for low-power, flexible, and wearable sensing applications. In addition, Wang *et al.* reported the development of a high-performance printed graphene-based antenna operating at 2.4 GHz.<sup>172</sup> Graphene conductive ink was synthesized using a liquid-phase exfoliation technique and printed onto water-transferable paper using a blade printing method. Subsequently, the printed design was transformed into a dipole antenna and transferred onto desired substrates. The performance of this graphene antenna met the requirements for IoT applications, suggesting its potential to serve as an alternative to traditional metallic antennas.

To enable longer read and write distances, faster speeds, and increased information storage capacity, researchers have explored the development of ultrahigh-frequency (UHF) technology. Colella *et al.* presented a 3D-printed UHF circularly polarized antenna, integrated with a specifically designed Wi-Fi-RFID reader for wearable biomedical applications.<sup>173</sup> These studies have opened up new avenues for antenna design in high-frequency operating range applications.

Moreover, special radio frequency (RF) antennas capable of operating in different frequency ranges have been developed. Li *et al.* fabricated large-area electrodes with excellent conductivity and optical transparency using screen printing and xenon flash-light sintering (FLS) techniques.<sup>174</sup> They also developed a multi-frequency RF antenna capable of operating in Wi-Fi, Bluetooth, and 5G bands. These advancements have practical implications for a wide range of applications. In terms of practical application, Niu *et al.* described the development of a body network comprising chip-free and battery-free elastic on-skin sensor tags that wirelessly connect to a flexible readout circuit.<sup>175</sup> Additionally, they proposed an innovative RF identification method wherein wireless sensors are intentionally detuned to enhance their tolerance to strain-induced changes in electrical characteristics. These findings contribute to the advancement of wireless sensor systems and their practical implementation.

## 6.2. NFC

In addition to RFID, NFC is another short distance wireless communication that facilitates information transmission between mobiles and terminals. The NFC labels can be activated *via* wireless power transmission by rectifying the coupled NFC carrier signal using a smartphone, which provides the advantages of lower power consumption and convenient applications in daily life.<sup>176</sup> He *et al.* have presented a biomimetic NFC antenna fabricated by a 3D direct-write printing method with a bionic spider-web structure, which had better stability under deformation (Fig. 7a).<sup>177</sup> Owing to excellent electromag-

netic and mechanical properties, the applications of the antenna were demonstrated in both emulated blood vessels and smart clothing, which have considerable potential in wearable and implantable electronics. In addition, Hakola *et al.* have demonstrated a paper-based electronic anti-counterfeiting label consisting of an NFC tag, an electrochromic display (ECD) module and circuitry *via* high-throughput R2R printing on a pilot scale (Fig. 7b).<sup>178</sup> The ECD component displays color change when in contact with an NFC device to indicate a genuine product. This work inspires the manufacture of sustainable electronics that are plastic-free and can be recycled. In another work, Sun *et al.* introduced an effective and affordable wireless anti-counterfeiting and item-tracking technology (Fig. 7c).<sup>42</sup> They employed an R2R printed NFC code label combined with quick response (QR) codes and a unified platform utilizing blockchain technology. The antennas were printed using Ag nanoparticle ink. Apart from this, the code generator, DC voltage tripler and supercapacitors in the integrated label were all fabricated in printable strategies. This work enables manufacturers, distributors, and market administrators to input all transaction information into the system. By scanning the illuminated QR code, customers can use their mobile phones to access real-time and accurate information by connecting to the blockchain. Such NFC labels can also be applied in food tracking. For example, Maskey *et al.* designed an R2R gravure-printed NFC antenna to function as a smart label for wireless monitoring of a food package time-temperature history.<sup>179</sup> In addition, Shao *et al.* achieved high-precision printing of flexible antennae at room temperature using additive-free MXene aqueous ink (Fig. 7d).<sup>41</sup> MXene inks exhibited excellent rheological and electrical properties, making them highly suitable for precise extrusion printing on various flat and curved substrates without the need for annealing. This approach also allowed for the easy fabrication of high-performance modules either independently or by integrating them with other electrical components, showing great potential for replacing cumbersome e-waste electronics such as commercial antennas. These studies highlight the potential of printable NFC labels for various applications, ranging from anti-counterfeiting labels to item tracking systems.

## 6.3. Others

In addition to RFID and NFC antennas, specialized antennas are also designed and employed for specific applications. For instance, in order to simultaneously fulfilling the requirements for near and far field communication, Luadang *et al.* utilized a planar inverted F antenna (PIFA) structure to integrate a far-field (FF) antenna with an NFC antenna.<sup>180</sup> This configuration enables efficient wireless communication in both short-range at 13.56 MHz and long-range communication in the frequency range of 1.8–2.1 GHz. In another work, Rahman *et al.* presented a wearable ultra-wideband (UWB) antenna designed primarily for brain stroke detection.<sup>181</sup> The antenna was implemented on a paper substrate by inkjet printing of copper nanoparticle inks in the form of a coplanar waveguide. It supports a remarkably wide bandwidth that covers



**Fig. 7** Printable fabrication of antennas on flexible substrates. (a) Stretchable NFC antenna with a spider-web serpentine structure based on the 3D direct-write printing method. Reproduced from ref. 177 with permission from [Elsevier], copyright [2023]. (b) NFC smart labels manufactured via the R2R printing method. Reproduced from ref. 178 with permission from [Springer Nature], copyright [2021]. (c) Fully printed multifunctional label with NFC wireless anti-counterfeiting and item-tracking. Reproduced from ref. 42 with permission from [John Wiley and Sons], copyright [2021]. (d) Fabrication and mechanism of printed MXene NFC tags. Reproduced from ref. 41 with permission from [Springer Nature], copyright [2022].

the 2.36–2.4 GHz medical body area network band, the 2.4–2.5 GHz industrial, scientific and medical band, and the 3.1–10.6 GHz UWB and so on. The broad frequency range makes it suitable for various applications in the medical field.

Overall, printable antennas allow versatile design form factors to fulfill the requirements of diverse communication scenarios, along with attractive properties such as light weight, low cost and sustainability. Table 3 summarizes some of the typical works on printable antennas according to different printing methods, materials, substrates, operating frequencies and other critical factors.

## 7. Printable integrated system for wireless healthcare applications

To realize wireless healthcare applications, it is necessary to associate sensors with wireless transmission circuits into a

fully integrated printable sensor system so as to facilitate convenient health status tracking.<sup>187</sup> Typically, health monitoring can be categorized into mainly two types: noninvasive and invasive/implantable. This section will focus on printable strategies to realize the integration of multi-functional modules into flexible and miniaturized platforms with robustness.

### 7.1. Noninvasive sensing systems

**Gas sensing.** Respiratory changes and volatile organic compounds in expiration/surroundings occurring in daily life can provide essential human health parameters for early disease diagnosis and human health assessment. For instance, Lin *et al.* successfully demonstrated a monolithically integrated self-powered intelligent sensor system that incorporates a printable gas sensor for ethanol and acetone detection (Fig. 8a).<sup>188</sup> Inkjet printing was employed to fabricate gas sensors, super-capacitors as energy storage modules and circuit interconnects. This approach allows for the seamless integration of

Table 3 Summary of the printable antennas

Type of antenna	Printing method	Printing material	Substrate	Key factor	Operating frequency	Ref.
RFID	Inkjet printing	Ag	PET	—	—	182
	Spray/dispense/contact printing	Graphene	Textiles	-	13.56 MHz	171
NFC	3D printing	Cu	PLA	—	865–868 MHz	183
	R2R	Ag	Polyimide (PI)	$Q = 4.1$	13.56 MHz	42
	R2R	Ag NP	PI	—	above 15.45 MHz	184
	R2R	Ag NP	PET/PI	$Q = 2.9$	13.56 MHz	179
Dipole antenna	Screen printing	Graphene	Paper	$Q = 0.65$	13.56 MHz	185
	Blade printing	Graphene	Paper	$S_{11} = -13.79$ dB	2.3–2.5 GHz	172
UWB antenna	Inkjet printing	Cu NP	Paper	$S_{11} = -10$ dB	1.91–34.45 GHz	186
Multi-frequency RF antenna	Screen printing	Ag NW	PET	$S_{11} < -10$ dB	0.71–1.25 and 1.73–2.16 GHz	174
Far-field/NFC	Screen printing	Ag	PET	$S_{11} < -6$ dB	13.56 MHz	180

different types of modules on flexible substrates. In another work, Mishra *et al.* developed fully integrated epidermal tattoo and textile-based nerve-agent vapor biosensor devices for continuous vapor-phase detection of organophosphate (OP) nerve-agent vapors.<sup>189</sup> Stress-enduring inks were used for the fabrication of stretchable organophosphorus hydrolase (OPH) enzyme electrodes. These wearable sensors were then coupled with flexible electronic platforms to enable wireless transmission of analytical data to mobile devices, sending warnings to the user of potential chemical dangers.

Overall, since the device architectures for individual gas sensors are relatively simple, it is quite straightforward to realize sensors by layer-by-layer printing. Since most of the targeted gas analytes for healthcare are at low concentrations, gas sensors based on printed dense films might generate relatively small output signals and could be interfered with humidity and other chemicals. Therefore, hardware designs play a significant role in achieving accurate signal decoding.

**Epidermal sensing.** Noninvasive sensor devices are also commonly applied for real-time extraction of biological signals. Wang *et al.* presented a printable temperature sensor by combining inkjet printing of Ag electrodes with dispensed printing of the PEDOT:PSS sensing layer and CYTOP passivation layer on top (Fig. 8b).<sup>153</sup> The sensor was integrated into with a printed flexible circuit for real-time body temperature monitoring. To achieve molecular level biomarker analysis, Nagamine *et al.* presented inkjet printed hydrogel-based chemical sensors that combine with the low-power Bluetooth protocol for *in situ* sweat L-lactate remote tracking.<sup>155</sup> Hydrocarbon-based solutions of Ag nanoparticles were prepared to fabricate working and reference electrode patterns. Similarly, Gillan *et al.* introduced miniaturized electrochemical sensors using high-throughput R2R fabrication for noninvasive, wireless real-time sweat lactate mapping on different body regions.<sup>190</sup>

Attractively, stretchable and elastic electronic skin can also be implemented in printable approaches. As illustrated in Fig. 8c, Byun *et al.* developed a fully printed, strain-engineered

electronic platform that allows customized multi-functional device integration. To realize stretchable interconnects, the key innovation lies in the structural optimization of the inkjet printed PMMA islands that were enclosed with the PDMS matrix. It also allows enhanced skin-conformability for wearable demonstrations including wrist movement sensing, self-computable digital logics and display.<sup>191</sup> Y. Song *et al.* reported a 3D direct printing technique to fabricate an epifluidic elastic electronic skin ( $e^3$ -skin) system with multimodal physico-chemical sensing capabilities (Fig. 8d).<sup>192</sup> This fully printable system consists of a series of electrochemical sweat biosensors and biophysical sensors, a microfluidic system for efficient sweat sampling, and a micro-supercapacitor (MSC) that were further integrated with wireless electronic modules. The custom-designed extrudable inks based on a variety of polymers and nanomaterials, such as Mxenes, play a critical role in efficient maskless 3D printing fabrication and the desirable mechanical robustness of the integrated systems.

## 7.2. Implantable sensing systems

Compared to noninvasive sensor systems, implantable devices can monitor the internal human environment with in-depth health information, while it poses high requirements on device miniaturization, seamlessly interfacing with tissues, materials biocompatibility and systematic design for reliable wireless communication.<sup>193</sup> Therefore, most of the implantable devices and systems are fabricated with traditional micro-electronic fabrication techniques, such as the complementary metal-oxide-semiconductor (CMOS) process. The advance in printable devices for such implantable sensing applications is in an early stage and requires further research efforts.

For cardiovascular disease diagnosis and monitoring, measuring the hemodynamic parameters such as pressure, flow rate and flow resistance is of great significance. In this regard, Herbert *et al.* presented a stretchable implantable bio-system for cerebral aneurysm hemodynamics monitoring.<sup>194</sup> As shown in Fig. 8e, stretchable capacitor sensors were prepared by aerosol jet printing and can be integrated with stents





**Fig. 8** Printable fabrication of integrated and wireless sensing systems for healthcare applications. (a) Schematic illustrations of the fully printable and monolithically integrated smart sensor system. Reproduced from ref. 188 with permission from [John Wiley and Sons], copyright [2018]. (b) A wireless real-time temperature sensing platform. Reproduced from ref. 153 with permission from [Springer Nature], copyright [2020]. (c) Printable and stretchable customized platform for wrist movement sensing. Reproduced from ref. 191 with permission from [Springer Nature], copyright [2017]. (d) 3D printed epifluidic elastic electronic skin ( $E^3$ ) for wireless physiological monitoring. Reproduced from ref. 192 with permission from [American Association for the Advancement of Science], copyright [2023]. (e) Fully printed implantable hemodynamics monitoring biosystems. Reproduced from ref. 194 with permission from [John Wiley and Sons], copyright [2019]. (f) Schematic illustration and images of implantable sensing systems based on ultrasonic energy transfer and communication. Reproduced from ref. 195 with permission from [American Association for the Advancement of Science], copyright [2021].

to be implanted into blood vessels. The system can be operated in a batteryless and wireless manner *via* inductive coupling of coils. Similarly, they also demonstrated a wireless vascular electronic system with a fully aerosol jet-printed soft sensor to monitor arterial pressure, pulse rate and flow rate. It is highly expected that printed antennas and supporting circuitry

can be further explored to be compatibly and seamlessly integrated with such printed sensors, so as to realize fully printable implantable sensing systems with desirable miniaturized sizes and mechanical robustness.

Apart from utilizing antennas for batteryless and wireless sensing, ultrasonic energy transfer and communication

technology has emerged as an attractive and convenient strategy for implantable devices in recent years. For instance, Jin *et al.* developed a soft, adaptable and battery-free implantable system based on flexible transducer arrays (Fig. 8f).<sup>195</sup> Casting molds for ultrasonic focusing launchers were prepared by high-resolution 3D printing. Besides, screen printing was adopted to fill solder paste efficiently for convenient connection between metal interconnects and chip components.

The future developments of printable and wireless integrated systems for implantable applications hold great potential in revolutionizing the healthcare industry. By combining facile and cost-effective printing technologies, personalized and miniaturized devices with lower costs can be achieved to enhance the clinical treatment effectiveness and improve the living quality.<sup>196</sup> However, implantable devices would pose strict requirements on printable materials and printing resolution to precisely construct micro/nanostructures.<sup>197</sup> Future developments of printable and wireless integrated systems are expected to focus on material engineering with biocompatibility and long-term duration, printing accuracy and scalability, as well as standard criteria and privacy regulation.

To meet the increasing demand for both wearable and implantable healthcare devices, it is essential to create sensors and supporting modules that exhibit specific characteristics, such as miniaturized size, robust integration and encapsulation, without a high manufacturing cost. Additionally, incorporating machine learning can enhance signal processing and recognition accuracy while maintaining signal decoding reliability. However, it still remains quite challenging to achieve fully printable fabrication of integrated electronics for wireless health.

## 8. Conclusion and outlook

In recent years, significant progress has been made in the field of printable electronics, particularly in the development of printable fabrication strategies for integrated sensing systems with wireless data transmission, catering to the needs of smart healthcare. Various sensors and printable antennas have been prepared for applications in remote health monitoring, human-computer interactions, and environmental monitoring. Some of these sensors exhibit high stability and sensitivity, making them ideal candidates for integration into complete sensor systems.

This review provides an overview of printable sensor devices with wireless data transmission, starting with an introduction to commonly adopted printing technologies, inks, and substrates. It then highlights typical printable sensors and antennas, followed by the presentation of representative integrated sensor systems based on printable sensors and wireless circuits.

However, several challenges remain in the fabrication of wireless sensor systems. Firstly, the key performance evaluation factors, including the sensitivity and stability of printable sensors, are still less competitive. They often experience decayed performances under mechanical interference or

during long-term usage, mainly due to less robustness in printed thin film sensing layers and interfaces. For chemical sensors, exposure to biological fluids can lead to biological contamination, chemical changes, or irreversible non-specific adsorption on the sensor surface. Secondly, reducing communication delay in wireless transmission systems is another important consideration. The communication delay depends on the specific communication technology employed. Real-time biofeedback systems require minimal communication delay, which necessitates the selection of appropriate antennas and optimization of wireless communication circuits.<sup>198</sup> Thirdly, as the size of integrated sensing systems continues to be miniaturized, achieving high-level integration becomes crucial. Integrating sensors with other electronic devices and power supply modules into a single flexible platform is a challenge that needs to be addressed. The monolithic integration strategy would ensure mechanical robustness and operational reliability while minimizing signal noises.

In summary, the advances of printable and flexible integrated sensing systems have attracted research interest from interdisciplinary fields, including materials science, electrical engineering and mechanical engineering. Research efforts are expected to emphasize rational engineering on printable materials, electrode patterns/interconnects structural innovation to tackle the existing challenges. There is no doubt that such integrated sensing electronics that can be manufactured in a printable manner will provide feasible, customized, cost-effective and reliable platforms for wireless healthcare.

## Conflicts of interest

The authors declare no conflict of interest.

## Acknowledgements

This work was supported by the National Natural Science Foundation of China (62201243), the Natural Science Foundation of Guangdong Province (2022A1515011928), the Fundamental and Applied Research Grant of Guangdong Province (2021A1515110627) and the Shenzhen Stable Support Plan Program for Higher Education Institutions Research Program (20220815153728002).

## References

- 1 Y. Luo, M. R. Abidian, J.-H. Ahn, D. Akinwande, A. M. Andrews, M. Antonietti, Z. Bao, M. Berggren, C. A. Berkey, C. J. Bettinger, J. Chen, P. Chen, W. Cheng, X. Cheng, S.-J. Choi, A. Chortos, C. Dagdeviren, R. H. Dauskardt, C.-A. Di, M. D. Dickey, X. Duan, A. Facchetti, Z. Fan, Y. Fang, J. Feng, X. Feng, H. Gao, W. Gao, X. Gong, C. F. Guo, X. Guo, M. C. Hartel, Z. He, J. S. Ho, Y. Hu, Q. Huang, Y. Huang, F. Huo, M. M. Hussain, A. Javey, U. Jeong, C. Jiang, X. Jiang,

- J. Kang, D. Karnaushenko, A. Khademhosseini, D.-H. Kim, I.-D. Kim, D. Kireev, L. Kong, C. Lee, N.-E. Lee, P. S. Lee, T.-W. Lee, F. Li, J. Li, C. Liang, C. T. Lim, Y. Lin, D. J. Lipomi, J. Liu, K. Liu, N. Liu, R. Liu, Y. Liu, Y. Liu, Z. Liu, Z. Liu, X. J. Loh, N. Lu, Z. Lv, S. Magdassi, G. G. Malliaras, N. Matsuhisa, A. Nathan, S. Niu, J. Pan, C. Pang, Q. Pei, H. Peng, D. Qi, H. Ren, J. A. Rogers, A. Rowe, O. G. Schmidt, T. Sekitani, D.-G. Seo, G. Shen, X. Sheng, Q. Shi, T. Someya, Y. Song, E. Stavrinidou, M. Su, X. Sun, K. Takei, X.-M. Tao, B. C. K. Tee, A. V.-Y. Thean, T. Q. Trung, C. Wan, H. Wang, J. Wang, M. Wang, S. Wang, T. Wang, Z. L. Wang, P. S. Weiss, H. Wen, S. Xu, T. Xu, H. Yan, X. Yan, H. Yang, L. Yang, S. Yang, L. Yin, C. Yu, G. Yu, J. Yu, S.-H. Yu, X. Yu, E. Zamburg, H. Zhang, X. Zhang, X. Zhang, X. Zhang, Y. Zhang, Y. Zhang, S. Zhao, X. Zhao, Y. Zheng, Y.-Q. Zheng, Z. Zheng, T. Zhou, B. Zhu, M. Zhu, R. Zhu, Y. Zhu, Y. Zhu, G. Zou and X. Chen, *ACS Nano*, 2023, **17**, 5211–5295.
- 2 Y. Zhou, X. Qiu, Z. A. Wan, Z. Long, S. Poddar, Q. Zhang, Y. Ding, C. L. J. Chan, D. Zhang, K. Zhou, Y. Lin and Z. Fan, *Nano Energy*, 2022, **100**, 107516.
- 3 X. Zeng, R. Peng, Z. Fan and Y. Lin, *Mater. Today Energy*, 2022, **23**, 100900.
- 4 L. Gu, S. Poddar, Y. Lin, Z. Long, D. Zhang, Q. Zhang, L. Shu, X. Qiu, M. Kam, A. Javey and Z. Fan, *Nature*, 2020, **581**, 278–282.
- 5 J. Zhao, H. Y. Y. Nyein, L. Hou, Y. Lin, M. Bariya, C. H. Ahn, W. Ji, Z. Fan and A. Javey, *Adv. Mater.*, 2021, **33**, 2006444.
- 6 L.-C. Tai, C. H. Ahn, H. Y. Y. Nyein, W. Ji, M. Bariya, Y. Lin, L. Li and A. Jamey, *ACS Sens.*, 2020, **5**, 1831–1837.
- 7 X. Ma, R. Peng, W. Mao, Y. Lin and H. Yu, *Electrochem. Sci. Adv.*, 2023, **3**, e2100163.
- 8 Y. Shi, Z. Zhang, Q. Huang, Y. Lin and Z. Zheng, *J. Semicond.*, 2023, **44**, 021601.
- 9 W. A. D. M. Jayathilaka, K. Qi, Y. Qin, A. Chinnappan, W. Serrano-Garcia, C. Baskar, H. Wang, J. He, S. Cui, S. W. Thomas and S. Ramakrishna, *Adv. Mater.*, 2019, **31**, 1805921.
- 10 W. S. Lee, S. Jeon and S. J. Oh, *Nano Convergence*, 2019, **6**, 1–13.
- 11 B. Ramachandran and Y.-C. Liao, *Biomicrofluidics*, 2022, **16**, 0116648.
- 12 X. Ma, P. Wang, L. Huang, R. Ding, K. Zhou, Y. Shi, F. Chen, Q. Zhuang, Q. Huang, Y. Lin and Z. Zheng, *Sci. Adv.*, 2023, **9**, 2763–2763.
- 13 X. Ma, Z. Jiang and Y. Lin, *J. Semicond.*, 2021, **42**, 101602.
- 14 X. Sun, C. Zhao, H. Li, H. Yu, J. Zhang, H. Qiu, J. Liang, J. Wu, M. Su, Y. Shi and L. Pan, *Micromachines*, 2022, **13**, 784.
- 15 H. Landaluce, L. Arjona, A. Perallos, F. Falcone, I. Angulo and F. Muralter, *Sensors*, 2020, **20**, 2495.
- 16 S. K. Behera, *IEEE Sens. J.*, 2022, **22**, 1105–1120.
- 17 Z. Cao, P. Chen, Z. Ma, S. Li, X. Gao, R.-X. Wu, L. Pan and Y. Shi, *Sensors*, 2019, **19**, 3947.
- 18 Y. Sun, N. Liu, Z. Yu and Y. Zhou, *Chin. J. Sci. Instrum.*, 2020, **41**, 122–137.
- 19 S. Figueroa Lorenzo, J. Anorga Benito, P. Garcia Cardarelli, J. Alberdi Garaia and S. Arrizabalaga Juaristi, *Technologies*, 2019, **7**, 15.
- 20 P. Swetha, U. Balijapalli and S.-P. Feng, *Electrochem. Commun.*, 2022, **140**, 107314.
- 21 Y. Yang, X. Guo, M. Zhu, Z. Sun, Z. Zhang, T. He and C. Lee, *Adv. Energy Mater.*, 2023, **13**, 2203040.
- 22 Q. Shi, B. Dong, T. He, Z. Sun, J. Zhu, Z. Zhang and C. Lee, *InfoMat*, 2020, **2**, 1131–1162.
- 23 S. Faham, A. Salimi and R. Ghavami, *Talanta*, 2023, **253**, 123892.
- 24 Z. Song, W. Ye, Z. Chen, Z. Chen, M. Li, W. Tang, C. Wang, Z. A. Wan, S. Poddar, X. Wen, X. Pan, Y. Lin, Q. Zhou and Z. Fan, *ACS Nano*, 2021, **15**, 7659–7667.
- 25 J. Zhao, Y. Lin, J. Wu, H. Y. Y. Nyein, M. Bariya, L.-C. Tai, M. Chao, W. Ji, G. Zhang, Z. Fan and A. Javey, *ACS Sens.*, 2019, **4**, 1925–1933.
- 26 J. R. Camargo, L. O. Orzari, D. A. G. Araujo, P. R. de Oliveira, C. Kalinke, D. P. Rocha, A. L. dos Santos, R. M. Takeuchi, R. A. A. Munoz, J. A. Bonacin and B. C. Janegitz, *Microchem. J.*, 2021, **164**, 105998.
- 27 X. Du, S. P. Wankhede, S. Prasad, A. Shehri, J. Morse and N. Lakal, *J. Mater. Chem. C*, 2022, **10**, 14091–14115.
- 28 L. Liu, H. Huang, X. Wang, P. He and J. Yang, *J. Phys. D: Appl. Phys.*, 2022, **55**, 283002.
- 29 D. Maddipatla, B. B. Narakathu and M. Atashbar, *Biosensors*, 2020, **10**, 10120199.
- 30 P. Yanez-Sedeno, S. Campuzano and J. M. Pingarron, *Biosensors*, 2020, **10**, 10070076.
- 31 B. Wang, M. Gao, X. Fu, M. Geng, Y. Liu, N. Cheng, J. Li, L. Li, Z. Zhang and Y. Song, *Nano Energy*, 2023, **107**, 108135.
- 32 C. Zhang, L. Zhang, Z. Pu, B. Bao, W. Ouyang and D. Li, *Nano Energy*, 2023, **113**, 108574.
- 33 S. Zhang, S. M. S. Rana, T. Bhatta, G. B. Pradhan, S. Sharma, H. Song, S. Jeong and J. Y. Park, *Nano Energy*, 2023, **106**, 108110.
- 34 Y. Lin, Y. Gao, F. Fang and Z. Fan, *Nano Res.*, 2018, **11**, 3065–3087.
- 35 M. Sun, J. Lv, H. Xu, L. Zhang, Y. Zhong, Z. Chen, X. Sui, B. Wang, X. Feng and Z. Mao, *Cellulose*, 2020, **27**, 2939–2952.
- 36 M. Bariya, Z. Shahpar, H. Park, J. Sun, Y. Jung, W. Gao, H. Y. Y. Nyein, T. S. Liaw, L.-C. Tai, Q. P. Ngo, M. Chao, Y. Zhao, M. Hettick, G. Cho and A. Javey, *ACS Nano*, 2018, **12**, 6978–6987.
- 37 Y. Sui, Y. Dai, C. C. Liu, R. M. Sankaran and C. A. Zorman, *Adv. Mater. Technol.*, 2019, **4**, 1900119.
- 38 H. Lei, K. Cao, Y. Chen, Z. Liang, Z. Wen, L. Jiang and X. Sun, *Chem. Eng. J.*, 2022, **445**, 136821.
- 39 B. Zhu, Y. Ling, L. W. Yap, M. Yang, F. Lin, S. Gong, Y. Wang, T. An, Y. Zhao and W. Cheng, *ACS Appl. Mater. Interfaces*, 2019, **11**, 29014–29021.



- 40 R. K. Mishra, J. R. Sempionatto, Z. Li, C. Brown, N. M. Galdino, R. Shah, S. Liu, L. J. Hubble, K. Bagot, S. Tapert and J. Wang, *Talanta*, 2020, **211**, 120757.
- 41 Y. Shao, L. Wei, X. Wu, C. Jiang, Y. Yao, B. Peng, H. Chen, J. Huangfu, Y. Ying, C. J. Zhang and J. Ping, *Nat. Commun.*, 2022, **13**, 3223.
- 42 J. Sun, S. Parajuli, K. Shrestha, J. Park, S. Shrestha, Y. Jung, H. Park, G. R. Koirala, N. Nasir, S. Kim, H. Truong, H. Jang, J. Lee, J. Lee and G. Cho, *Adv. Mater. Technol.*, 2022, **7**, 2100969.
- 43 K. Mondal and M. D. McMurtrey, *Mater. Today Chem.*, 2020, **17**, 100328.
- 44 Q. Liu, B. Tian, J. Liang and W. Wu, *Mater. Horiz.*, 2021, **8**, 1634–1656.
- 45 A. M. Tiara, H. Moon, G. Cho and J. Lee, *Jpn. J. Appl. Phys.*, 2022, **61**, 0802.
- 46 R. Abbel, Y. Galagan and P. Groen, *Adv. Eng. Mater.*, 2018, **20**, 1701190.
- 47 Y. Choi, Y. Jung, R. Song, J. Park, S. Parajuli, S. Shrestha, G. Cho and B.-S. Kim, *Nanomaterials*, 2023, **13**, 590.
- 48 J. Lemarchand, N. Bridonneau, N. Battaglini, F. Carn, G. Mattana, B. Piro, S. Zrig and V. Noel, *Angew. Chem., Int. Ed.*, 2022, **61**, 202200166.
- 49 X. Shi, Z.-S. Wu and X. Bao, *Electrochem. Energy Rev.*, 2020, **3**, 581–612.
- 50 J. Liang, C. Jiang and W. Wu, *Appl. Phys. Rev.*, 2021, **8**, 021319.
- 51 W. Wu, *Nanoscale*, 2017, **9**, 7342–7372.
- 52 S. P. Sreenilayam, I. Ul Ahad, V. Nicolosi, V. A. Garzon and D. Brabazon, *Mater. Today*, 2020, **32**, 147–177.
- 53 B. Philip, E. Jewell, P. Greenwood and C. Weirman, *J. Manuf. Processes*, 2016, **22**, 185–191.
- 54 A. Gusain, A. Thankappan and S. Thomas, *J. Mater. Sci.*, 2020, **55**, 13490–13542.
- 55 H. W. Choi, T. Zhou, M. Singh and G. E. Jabbour, *Nanoscale*, 2015, **7**, 3338–3355.
- 56 X. Zhang, K. Liu, V. Sunappan and X. Shan, *J. Mater. Process. Technol.*, 2015, **225**, 337–346.
- 57 Z. W. Zhong, J. H. Ee, S. H. Chen and X. C. Shan, *Mater. Manuf. Processes*, 2020, **35**, 564–571.
- 58 S. H. Lee and S. Lee, *Int. J. Precis. Eng. Manuf. – Green Technol.*, 2022, **9**, 409–420.
- 59 H. Y. Y. Nyein, M. Bariya, L. Kivimaki, S. Uusitalo, T. S. Liaw, E. Jansson, C. H. Ahn, J. A. Hangasky, J. Zhao, Y. Lin, T. Happonen, M. Chao, C. Liedert, Y. Zhao, L.-C. Tai, J. Hiltunen and A. Javey, *Sci. Adv.*, 2019, **5**, 9906.
- 60 H. Abdolmaleki, P. Kidmose and S. Agarwala, *Adv. Mater.*, 2021, **33**, 2006792.
- 61 N. C. Raut and K. Al-Shamery, *J. Mater. Chem. C*, 2018, **6**, 1618–1641.
- 62 J. Li, F. Rossignol and J. Macdonald, *Lab Chip*, 2015, **15**, 2538–2558.
- 63 A. Al-Halhouli, H. Qitouqa, A. Alashqar and J. Abu-Khalaf, *Sens. Rev.*, 2018, **38**, 438–452.
- 64 T.-T. Huang and W. Wu, *J. Mater. Chem. A*, 2019, **7**, 23280–23300.
- 65 B. Derby, in *Annual Review of Materials Research*, ed. D. R. Clarke, M. Ruhle and F. Zok, 2010, vol. 40, pp. 395–414.
- 66 X. Li, B. Liu, B. Pei, J. Chen, D. Zhou, J. Peng, X. Zhang, W. Jia and T. Xu, *Chem. Rev.*, 2020, **120**, 10596–10636.
- 67 K. K. B. Hon, L. Li and I. M. Hutchings, *CIRP Ann. – Manuf. Technol.*, 2008, **57**, 601–620.
- 68 P. Yang and H. J. Fan, *Adv. Mater. Technol.*, 2020, **5**, 2000217.
- 69 E. Tekin, P. J. Smith and U. S. Schubert, *Soft Matter*, 2008, **4**, 703–713.
- 70 N. Reis, C. Ainsley and B. Derby, *J. Appl. Phys.*, 2005, **97**, 094903.
- 71 L. Liu, D. Xiang, Y. Wu, Z. Zhou, H. Li, C. Zhao and Y. Li, *Front. Mater.*, 2021, **8**, 725420.
- 72 M. A. Ali, C. Hu, E. A. Yttri and R. Panat, *Adv. Funct. Mater.*, 2022, **32**, 2107671.
- 73 M. Schouten, G. Wolterink, A. Dijkshoorn, D. Kosmas, S. Stramigioli and G. Krijnen, *IEEE Sens. J.*, 2021, **21**, 12900–12912.
- 74 H. Choudhary, D. Vaithyanathan and H. Kumar, *MAPAN*, 2021, **36**, 405–422.
- 75 J. T. Reeder, Y. Xue, D. Franklin, Y. Deng, J. Choi, O. Prado, R. Kim, C. Liu, J. Hanson, J. Cirraldo, A. J. Bandodkar, S. Krishnan, A. Johnson, E. Patnaude, R. Avila, Y. Huang and J. A. Rogers, *Nat. Commun.*, 2019, **10**, 5513.
- 76 G. L. Goh, H. Zhang, T. H. Chong and W. Y. Yeong, *Adv. Electron. Mater.*, 2021, **7**, 2100445.
- 77 M. Ntagios, H. Nassar, A. Pullanchiyodan, W. T. Navaraj and R. Dahiya, *Adv. Intell. Syst.*, 2020, **2**, 1900080.
- 78 Z. Pei, Q. Zhang, K. Yang, Z. Yuan, W. Zhang and S. Sang, *Adv. Mater. Technol.*, 2021, **6**, 2100038.
- 79 Z. Tang, S. Jia, C. Zhou and B. Li, *ACS Appl. Mater. Interfaces*, 2020, **12**, 28669–28680.
- 80 T. Kim, Q. Yi, E. Hoang and R. Esfandyarpour, *Adv. Mater. Technol.*, 2021, **6**, 2001021.
- 81 Z. Zhu, H. S. Park and M. C. McAlpine, *Sci. Adv.*, 2020, **6**, 5575.
- 82 T. Tuan Sang, N. K. Dutta and N. R. Choudhury, *Adv. Colloid Interface Sci.*, 2018, **261**, 41–61.
- 83 Y. H. Wang, D. X. Du, H. Xie, X. B. Zhang, K. W. Lin, K. Wang and E. Fu, *J. Mater. Sci.: Mater. Electron.*, 2021, **32**, 496–508.
- 84 Z. Chu, J. Peng and W. Jin, *Sens. Actuators, B*, 2017, **243**, 919–926.
- 85 K. Rajan, I. Roppolo, A. Chiappone, S. Bocchini, D. Perrone and A. Chiolerio, *Nanotechnol., Sci. Appl.*, 2016, **9**, 1–13.
- 86 S. Xu and W. Wu, *Adv. Intell. Syst.*, 2020, **2**, 2000117.
- 87 D. Li, W.-Y. Lai, Y.-Z. Zhang and W. Huang, *Adv. Mater.*, 2018, **30**, 1704738.
- 88 C. S. Boland, U. Khan, H. Benameur and J. N. Coleman, *Nanoscale*, 2017, **9**, 18507–18515.
- 89 X. Xu, G. Han, H. Yu, X. Jin, J. Yang, J. Lin and C. Ma, *J. Phys. D: Appl. Phys.*, 2020, **53**, 051t02.

- 90 B. Tian, W. Yao, P. Zeng, X. Li, H. Wang, L. Liu, Y. Feng, C. Luo and W. Wu, *J. Mater. Chem. C*, 2019, **7**, 809–818.
- 91 W. J. Hyun, S. Lim, B. Y. Ahn, J. A. Lewis, C. D. Frisbie and L. F. Francis, *ACS Appl. Mater. Interfaces*, 2015, **7**, 12619–12624.
- 92 H.-G. Im, S.-H. Jung, J. Jin, D. Lee, J. Lee, D. Lee, J.-Y. Lee, I.-D. Kim and B.-S. Bae, *ACS Nano*, 2014, **8**, 10973–10979.
- 93 J.-G. Lee, J.-H. Lee, S. An, D.-Y. Kim, T.-G. Kim, S. S. Al-Deyab, A. L. Yarin and S. S. Yoon, *J. Mater. Chem. A*, 2017, **5**, 6677–6685.
- 94 H.-S. Kim, Y. S. Seo, K. Kim, J. W. Han, Y. Park and S. Cho, *Nanoscale Res. Lett.*, 2016, **11**, 230.
- 95 N. P. Bacalzo Jr., L. P. Go, C. J. Querebillo, P. Hildebrandt, F. T. Limpoco and E. P. Enriquez, *ACS Appl. Nano Mater.*, 2018, **1**, 1247–1256.
- 96 P. Pienpinijtham, C. Thammacharoen and S. Ekgasit, *Macromol. Res.*, 2012, **20**, 1281–1288.
- 97 J. Rodriguez-Fernandez, J. Perez-Juste, F. Javier Garcia de Abajo and L. M. Liz-Marzan, *Langmuir*, 2006, **22**, 7007–7010.
- 98 H. He, R. Chen, L. Zhang, T. Williams, X. Fang and W. Shen, *J. Colloid Interface Sci.*, 2020, **562**, 333–341.
- 99 N. A. Luechinger, E. K. Athanassiou and W. J. Stark, *Nanotechnology*, 2008, **19**, 445201.
- 100 C. Lee, N. R. Kim, J. Koo, Y. J. Lee and H. M. Lee, *Nanotechnology*, 2015, **26**, 455601.
- 101 X. Yu, J. Li, T. Shi, C. Cheng, G. Liao, J. Fan, T. Li and Z. Tang, *J. Alloys Compd.*, 2017, **724**, 365–372.
- 102 E. B. Choi and J.-H. Lee, *Appl. Surf. Sci.*, 2019, **480**, 839–845.
- 103 Y. Zhang, P. Zhu, G. Li, Z. Cui, C. Cui, K. Zhang, J. Gao, X. Chen, G. Zhang, R. Sun and C. Wong, *ACS Appl. Mater. Interfaces*, 2019, **11**, 8382–8390.
- 104 T. G. Kim, H. J. Park, K. Woo, S. Jeong, Y. Choi and S. Y. Lee, *ACS Appl. Mater. Interfaces*, 2018, **10**, 1059–1066.
- 105 M. Grouchko, A. Kamysny and S. Magdassi, *J. Mater. Chem.*, 2009, **19**, 3057–3062.
- 106 J. Perelaer, B.-J. de Gans and U. S. Schubert, *Adv. Mater.*, 2006, **18**, 2101.
- 107 H. Jiang, L. Zheng, Z. Liu and X. Wang, *InfoMat*, 2020, **2**, 1077–1094.
- 108 G. Hu, J. Kang, L. W. T. Ng, X. Zhu, R. C. T. Howe, C. G. Jones, M. C. Hersam and T. Hasan, *Chem. Soc. Rev.*, 2018, **47**, 3265–3300.
- 109 K. Pan, Y. Fan, T. Leng, J. Li, Z. Xin, J. Zhang, L. Hao, J. Gallop, K. S. Novoselov and Z. Hu, *Nat. Commun.*, 2018, **9**, 5197.
- 110 A. S. Pavlova, E. A. Obraztsova, A. V. Belkin, C. Monat, P. Rojo-Romeo and E. D. Obraztsova, *J. Nanophotonics*, 2016, **10**, 012525.
- 111 V. Nicolosi, M. Chhowalla, M. G. Kanatzidis, M. S. Strano and J. N. Coleman, *Science*, 2013, **340**, 1420.
- 112 M. Yi and Z. Shen, *J. Mater. Chem. A*, 2015, **3**, 11700–11715.
- 113 M. Lotya, P. J. King, U. Khan, S. De and J. N. Coleman, *ACS Nano*, 2010, **4**, 3155–3162.
- 114 T. S. Tran, S. J. Park, S. S. Yoo, T.-R. Lee and T. Kim, *RSC Adv.*, 2016, **6**, 12003–12008.
- 115 D. S. Kim, J.-M. Jeong, H. J. Park, Y. K. Kim, K. G. Lee and B. G. Choi, *Nano-Micro Lett.*, 2021, **13**, 87.
- 116 K. Parvez, R. Worsley, A. Alieva, A. Felten and C. Casiraghi, *Carbon*, 2019, **149**, 213–221.
- 117 X. Liang, H. Li, J. Dou, Q. Wang, W. He, C. Wang, D. Li, J.-M. Lin and Y. Zhang, *Adv. Mater.*, 2020, **32**, 2000165.
- 118 J. O. Akindoyo, N. H. Ismail and M. Mariatti, *J. Mater. Sci.: Mater. Electron.*, 2021, **32**, 12648–12660.
- 119 J. Sun, R. Sun, P. Jia, M. Ma and Y. Song, *J. Mater. Chem. C*, 2022, **10**, 9441–9464.
- 120 T. Vinh Van, S. Lee, D. Lee and L. Thanh-Hai, *Polymers*, 2022, **14**, 3730.
- 121 S. Zhang, Y. Chen, H. Liu, Z. Wang, H. Ling, C. Wang, J. Ni, B. C. Saltik, X. Wang, X. Meng, H.-J. Kim, A. Baidya, S. Ahadian, N. Ashammakhi, M. R. Dokmeci, J. Travas-Sejdic and A. Khademhosseini, *Adv. Mater.*, 2020, **32**, 1904752.
- 122 V. R. Feig, H. Tran, M. Lee and Z. Bao, *Nat. Commun.*, 2018, **9**, 2740.
- 123 J. Rivnay, S. Inal, B. A. Collins, M. Sessolo, E. Stavrinidou, X. Strakosas, C. Tassone, D. M. Delongchamp and G. G. Malliaras, *Nat. Commun.*, 2016, **7**, 11287.
- 124 A. Corletto and J. G. Shapter, *J. Mater. Chem. C*, 2021, **9**, 14161–14174.
- 125 T. Ren, H. Yang, J. Zhang, K. Lv, D. Kong, F. Jiang, Y. Chang, P. Yu, J. Tao, D. Wang, N. Kong and Y. Shao, *Adv. Eng. Mater.*, 2023, **25**, 2301018.
- 126 R. Luo, X. Li, H. Li, B. Du and S. Zhou, *Prog. Org. Coat.*, 2022, **162**, 106593.
- 127 L.-W. Lo, J. Zhao, H. Wan, Y. Wang, S. Chakrabartty and C. Wang, *ACS Appl. Mater. Interfaces*, 2021, **13**, 21693–21702.
- 128 M. Prosa, M. Tassarolo, M. Bolognesi, T. Cramer, Z. Chen, A. Facchetti, B. Fraboni, M. Seri, G. Ruani and M. Muccini, *Adv. Mater. Interfaces*, 2016, **3**, 1600770.
- 129 U. Kraft, F. Molina-Lopez, D. Son, Z. Bao and B. Murmann, *Adv. Electron. Mater.*, 2020, **6**, 1900681.
- 130 D. D. C. Rasi, P. M. J. G. van Thiel, H. Bin, K. H. Hendriks, G. H. L. Heintges, M. M. Wienk, T. Becker, Y. Li, T. Riedl and R. A. J. Janssen, *Sol. RRL*, 2019, **3**, 1800366.
- 131 E. K. Arora, V. Sharma, A. Ravi, A. Shahi, S. Jagtap, A. Adhikari, J. K. Dash, P. Kumar and R. Patel, *Energies*, 2023, **16**, 6716.
- 132 S. Choudhury, D. Deepak, G. Bhattacharya, J. McLaughlin and S. S. Roy, *Macromol. Mater. Eng.*, 2023, **2300007**.
- 133 K. A. Saraswathi, M. S. B. Reddy, N. Jayarambabu, S. Aich and T. V. Rao, *Mater. Lett.*, 2023, **349**, 134850.
- 134 Y. Zhao, Y. Yu, S. Zhao, R. Zhu, J. Zhao and G. Cui, *Microchem. J.*, 2023, **185**, 108092.
- 135 C. Zhu, H. Xue, H. Zhao, T. Fei, S. Liu, Q. Chen, B. Gao and T. Zhang, *Talanta*, 2022, **242**, 123289.

- 136 E. Bilbao, S. Kapadia, V. Riechert, J. Amalvy, F. N. Molinari, M. M. Escobar, R. R. Baumann and L. N. Monsalve, *Sens. Actuators, B*, 2021, **346**, 130558.
- 137 M. Zea, R. Texido, R. Villa, S. Borros and G. Gabriel, *ACS Appl. Mater. Interfaces*, 2021, **13**, 33524–33535.
- 138 H. Ervasti, T. Jarvinen, O. Pitkanen, E. Bozo, J. Hiitola-Keinanen, O.-H. Huttunen, J. Hiltunen and K. Kordas, *ACS Appl. Mater. Interfaces*, 2021, **13**, 27284–27294.
- 139 A. Khan, K. Rahman, S. Ali, S. Khan, R. Wang and A. Bermak, *J. Mater. Res.*, 2021, **36**, 3568–3578.
- 140 M. T. Rahman, C.-Y. Chen, B. Karagoz, M. Renn, M. Schrandt, A. Gellman and R. Panat, *ACS Appl. Nano Mater.*, 2019, **2**, 3280–3291.
- 141 S. Agarwala, G. L. Goh, L. Truong-Son Dinh, J. An, Z. K. Peh, W. Y. Yeong and Y.-J. Kim, *ACS Sens.*, 2019, **4**, 218–226.
- 142 J. Wang, C. Lu and K. Zhang, *Energy Environ. Mater.*, 2020, **3**, 80–100.
- 143 R. Cao, X. Pu, X. Du, W. Yang, J. Wang, H. Guo, S. Zhao, Z. Yuan, C. Zhang, C. Li and Z. L. Wang, *ACS Nano*, 2018, **12**, 5190–5196.
- 144 J.-W. Lee, Y. Choi, J. Jang, S.-H. Yeom, W. Lee and B.-K. Ju, *Sens. Actuators, A*, 2020, **313**, 112205.
- 145 D. Barmpakos, C. Tsamis and G. Kaltsas, *Microelectron. Eng.*, 2020, **225**, 111266.
- 146 Z. Deng, T. Hu, Q. Lei, J. He, P. X. Ma and B. Guo, *ACS Appl. Mater. Interfaces*, 2019, **11**, 6796–6808.
- 147 X.-Y. Yin, Y. Zhang, X. Cai, Q. Guo, J. Yang and Z. L. Wang, *Mater. Horiz.*, 2019, **6**, 767–780.
- 148 J. Gao, Y. Fan, Q. Zhang, L. Luo, X. Hu, Y. Li, J. Song, H. Jiang, X. Gao, L. Zheng, W. Zhao, Z. Wang, W. Ai, Y. Wei, Q. Lu, M. Xu, Y. Wang, W. Song, X. Wang and W. Huang, *Adv. Mater.*, 2022, **34**, 2107511.
- 149 Y. Li, Y. Wei, Y. Yang, L. Zheng, L. Luo, J. Gao, H. Jiang, J. Song, M. Xu, X. Wang and W. Huang, *Research*, 2022, **2022**, 0002.
- 150 J. Sato, T. Sekine, W. Yi-Fei, Y. Takeda, H. Matsui, D. Kumaki, F. D. Dos Santos, A. Miyabo and S. Tokito, *Sens. Actuators, A*, 2019, **295**, 93–98.
- 151 Y. Yang, H. Wang, Y. Hou, S. Nan, Y. Di, Y. Dai, F. Li and J. Zhang, *Compos. Sci. Technol.*, 2022, **226**, 109518.
- 152 W. Li, M. Xu, J. Gao, X. Zhang, H. Huang, R. Zhao, X. Zhu, Y. Yang, L. Luo, M. Chen, H. Ji, L. Zheng, X. Wang and W. Huang, *Adv. Mater.*, 2023, **35**, 2207447.
- 153 Y.-F. Wang, T. Sekine, Y. Takeda, K. Yokosawa, H. Matsui, D. Kumaki, T. Shiba, T. Nishikawa and S. Tokito, *Sci. Rep.*, 2020, **10**, 2467.
- 154 Y. Lin, M. Bariya, H. Y. Y. Nyein, L. Kivimaki, S. Uusitalo, E. Jonsson, W. Ji, Z. Yuan, T. Happonen, C. Liedert, J. Hiltunen, Z. Fan and A. Javey, *Adv. Funct. Mater.*, 2019, **29**, 1902521.
- 155 K. Nagamine, T. Mano, A. Nomura, Y. Ichimura, R. Izawa, H. Furusawa, H. Matsui, D. Kumaki and S. Tokito, *Sci. Rep.*, 2019, **9**, 1–8.
- 156 S. A. Goodchild, L. J. Hubble, R. K. Mishra, Z. Li, K. Y. Goud, A. Barfidokht, R. Shah, K. S. Bagot, A. J. S. McIntosh and J. Wang, *Anal. Chem.*, 2019, **91**, 3747–3753.
- 157 R. Jin, D. Kong, X. Zhao, H. Li, X. Yan, F. Liu, P. Sun, D. Du, Y. Lin and G. Lu, *Biosens. Bioelectron.*, 2019, **141**, 111473.
- 158 J. Liu, X. Jiang, R. Zhang, Y. Zhang, L. Wu, W. Lu, J. Li, Y. Li and H. Zhang, *Adv. Funct. Mater.*, 2019, **29**, 1807326.
- 159 D. Lv, W. Chen, W. Shen, M. Peng, X. Zhang, R. Wang, L. Xu, W. Xu, W. Song and R. Tan, *Sens. Actuators, B*, 2019, **298**, 126890.
- 160 G. Manjunath, P. Nagaraju and S. Mandal, *J. Mater. Sci.: Mater. Electron.*, 2021, **32**, 5713–5728.
- 161 C. Li, J. Xiong, C. Zheng and J. Zhao, *ACS Appl. Nano Mater.*, 2022, **5**, 16655–16663.
- 162 S. Tajik, H. Beitollahi, S. A. Ahmadi, M. B. Askari and A. Di Bartolomeo, *Nanomaterials*, 2021, **11**, 3208.
- 163 K. Shrestha, Y. Kim, Y. Jung, S. Kim, H. Truong and G. Cho, *Flexible Printed Electron.*, 2021, **6**, 044001.
- 164 C. Liedert, L. Rannaste, A. Kokkonen, O.-H. Huttunen, R. Liedert, J. Hiltunen and L. Hakalahti, *ACS Sens.*, 2020, **5**, 2010–2017.
- 165 Y.-S. Huang, K.-Y. Chen, Y.-T. Cheng, C.-K. Lee and H.-E. Tsai, *IEEE Electron Device Lett.*, 2020, **41**, 597–600.
- 166 L.-W. Lo, H. Shi, H. Wan, Z. Xu, X. Tan and C. Wang, *Adv. Mater. Technol.*, 2020, **5**, 1900717.
- 167 P. B. Deroco, D. Wachholz Junior and L. T. Kubota, *Chemosensors*, 2021, **9**, 61.
- 168 S. I. Kim, H. Y. Jung, S. Yang, J. Yoon, H. Lee and W. Ryu, *Virtual Phys. Prototyping*, 2022, **17**, 156–169.
- 169 A. G. G. Samarentsis, G. Makris, S. Spinthaki, G. Christodoulakis, M. Tsiknakis and A. K. K. Pantazis, *Sensors*, 2022, **22**, 9725.
- 170 J. Kim, G. A. Salvatore, H. Araki, A. M. Chiarelli, Z. Xie, A. Banks, X. Sheng, Y. Liu, J. W. Lee, K.-I. Jang, S. Y. Heo, K. Cho, H. Luo, B. Zimmerman, J. Kim, L. Yan, X. Feng, S. Xu, M. Fabiani, G. Gratton, Y. Huang, U. Paik and J. A. Rogers, *Sci. Adv.*, 2016, **2**, 1600418.
- 171 T. Delipinar, E. A. Ozek, C. E. Kaya, S. Tanyeli and M. K. Yapici and Ieee, *2020 IEEE International Conference on Flexible and Printable Sensors and Systems (FLEPS)*, 2020, pp. 1–4.
- 172 W. Wang, C. Ma, X. Zhang, J. Shen, N. Hanagata, J. Huangfu and M. Xu, *Sci. Technol. Adv. Mater.*, 2019, **20**, 870–875.
- 173 G. Muntoni, G. Montisci, G. A. Casula, F. P. Chietera, A. Michel, R. Colella, L. Catarinucci and G. Mazzarella, *IEEE Antennas Wireless Propag. Lett.*, 2020, **19**, 1118–1122.
- 174 W. Li, E. Yarali, A. Bakytbekov, T. D. Anthopoulos and A. Shamim, *Nanotechnology*, 2020, **31**, 395201.
- 175 S. Niu, N. Matsuhisa, L. Beker, J. Li, S. Wang, J. Wang, Y. Jiang, X. Yan, Y. Yun, W. Burnetts, A. S. Y. Poon, J. B. H. Tok, X. Chen and Z. Bao, *Nat. Electron.*, 2019, **2**, 361–368.
- 176 L. Lin, M. Dautta, A. Hajiaghajani, A. R. Escobar, P. Tseng and M. Khine, *Adv. Electron. Mater.*, 2021, **7**, 2000765.



- 177 Z. He, Y. Wang, H. Xiao, Y. Wu, X. Xia, S. Li, J. Liu, K. Huang, F. Wang, J. Shang, Y. Liu, H. Li, F. Li, S. Wang, G. Zhu and R.-W. Li, *Nano Energy*, 2023, **112**, 108461.
- 178 L. Hakola, E. Jansson, R. Futsch, T. Happonen, V. Thenot, G. Depres, A. Rougier and M. Smolander, *Int. J. Adv. Manuf. Technol.*, 2021, **117**, 2921–2934.
- 179 B. B. Maskey, K. Shrestha, J. Sun, H. Park, J. Park, S. Parajuli, S. Shrestha, Y. Jung, S. Ramasundaram, G. R. Koirala and G. Cho, *RSC Adv.*, 2020, **10**, 12407–12414.
- 180 B. Luadang, A. Sakonkanapong, S. Dentri, R. Pansomboon and C. Phongcharoenpanich, *IEEE Access*, 2019, **7**, 171966–171973.
- 181 M. A. Rahman, M. F. Hossain, M. Hossain and R. Ahmmed, *Egypt. Inf. J.*, 2020, **21**, 23–35.
- 182 G. Ponraj, W. L. Yeo, K. S. Kumar, M. S. Kalairaj, C. J. Cai and H. Ren and IeeeXian, PEOPLES R CHINA, 2021.
- 183 G. Muntoni, G. Montisci, G. A. Casula, F. P. Chietera, A. Michel, R. Colella, L. Catarinucci and G. Mazzarella, *IEEE Antennas Wireless Propag. Lett.*, 2020, **19**, 1118–1122.
- 184 B. B. Maskey, J. Sun, K. Shrestha, S. Kim, M. Park, Y. Kim, H. Park, S. Lee, Y. Han, J. Lee, Y. Majima, J. Kim, J. Lee, G. Bahk, G. R. Koirala and G. Cho, *IEEE Sens. J.*, 2020, **20**, 2106–2116.
- 185 T. Leng, K. Parvez, K. Pan, J. Ali, D. McManus, K. S. Novoselov, C. Casiraghi and Z. Hu, *2D Mater.*, 2020, **7**, 024004.
- 186 M. A. Rahman and M. F. Hossain, 2019 *International Conference on Computer, Communication, Chemical, Materials and Electronic Engineering (IC4ME2)*, 2019, pp. 1–6.
- 187 Y. Guo, X. Wei, S. Gao, W. Yue, Y. Li and G. Shen, *Adv. Funct. Mater.*, 2021, **31**, 2104288.
- 188 Y. Lin, J. Chen, M. M. Tavakoli, Y. Gao, Y. Zhu, D. Zhang, M. Kam, Z. He and Z. Fan, *Adv. Mater.*, 2019, **31**, 1804285.
- 189 R. K. Mishra, A. Martin, T. Nakagawa, A. Barfidokht, X. Lu, J. R. Sempionatto, K. M. Lyu, A. Karajic, M. M. Musameh, I. L. Kyratzis and J. Wang, *Biosens. Bioelectron.*, 2018, **101**, 227–234.
- 190 L. Gillan, T. Teerinen, M. Suhonen, L. Kivimaki and A. Alastalo, *Flexible Printed Electron.*, 2021, **6**, 034003.
- 191 J. Byun, B. Lee, E. Oh, H. Kim, S. Kim, S. Lee and Y. Hong, *Sci. Rep.*, 2017, **7**, 45328.
- 192 Y. Song, R. Y. Tay, J. Li, C. Xu, J. Min, E. S. Sani, G. Kim, W. Heng, I. Kim and W. Gao, *Sci. Adv.*, 2023, **9**, 6492.
- 193 R. Herbert, H.-R. Lim, S. Park, J.-H. Kim and W.-H. Yeo, *Adv. Healthcare Mater.*, 2021, **10**, 2100158.
- 194 R. Herbert, S. Mishra, H.-R. Lim, H. Yoo and W.-H. Yeo, *Adv. Sci.*, 2019, **6**, 1901034.
- 195 P. Jin, J. Fu, F. Wang, Y. Zhang, P. Wang, X. Liu, Y. Jiao, H. Li, Y. Chen, Y. Ma and X. Feng, *Sci. Adv.*, 2021, **7**, 2507.
- 196 G. Liu, Z. Lv, S. Batool, M.-Z. Li, P. Zhao, L. Guo, Y. Wang, Y. Zhou and S.-T. Han, *Small*, 2023, **19**, 2207879.
- 197 T. Lu, S. Ji, W. Jin, Q. Yang, Q. Luo and T.-L. Ren, *Sensors*, 2023, **23**, 2991.
- 198 A. Kos, V. Milutinovic and A. Umek, *Future Gener. Comput. Syst.*, 2019, **92**, 582–592.